Forest Ecology and Management 437 (2019) 70–86

Contents lists available at ScienceDirect

Forest Ecology and Management

journal homepage: www.elsevier.com/locate/foreco

# Forest structure and pattern vary by climate and landform across active-fire landscapes in the montane Sierra Nevada

Sean M.A. Jeronimo[a,*], Van R. Kane[a], Derek J. Churchill[b], James A. Lutz[c], Malcolm P. North[d], Gregory P. Asner[e], Jerry F. Franklin[a]

[a] School of Environmental and Forest Sciences, College of the Environment, University of Washington, Box 352100, Seattle, WA 98195, USA
[b] Washington State, Department of Natural Resources, Forest Health Division, Box 47037, Olympia, WA 98504, USA
[c] Wildland Resources Department, Quinney College of Natural Resources, Utah State University, 5230 Old Main Hill, Logan, UT 84322, USA
[d] USDA Forest Service Pacific Southwest Research Station, 1731 Research Park Dr., Davis, CA 95618, USA
[e] Center for Global Discovery and Conservation Science, Arizona State University, Tempe, AZ 85281, USA

ABSTRACT

Restoration of fire-dependent forests is often guided by reference conditions from forests with an active fire regime, thought to be resilient to current and future disturbances and stresses. Reference conditions are usually based on historical data or reconstruction, which greatly limits the scale and completeness of data that can be collected. In the Sierra Nevada of California, large areas with reintroduced active fire regimes coupled with extensive lidar data coverage provide the unique opportunity to develop a contemporary regional reference condition dataset across a wide gradient of biophysical conditions. We developed this dataset with a focus on three questions: (1) What is the geographic and environmental distribution of restored active-fire forest areas in the Sierra Nevada mixed-conifer zone? (2) What are the ranges of variation in forest structure and spatial patterns across reference areas? And (3) How do stand density, tree clumping, and canopy opening patterns vary by topography and climate in reference areas? We analyzed fire history and environmental conditions over 10.8 million ha, including 3.9 million ha in the Sierra Nevada mixed-conifer zone, and found 30,377 ha of restored active-fire areas. Although reference areas were distributed throughout the Sierra Nevada they were more abundant on National Park lands (81% of reference areas) than National Forest lands and were associated with higher lightning strike density. Lidar-measured ranges of variation in reference condition structure were broad, with tree densities of 6–320 trees $ha^{-1}$ (median 107 trees $ha^{-1}$), basal area of 0.01–113 $m^2$ $ha^{-1}$ (median 21 $m^2$ $ha^{-1}$), average size of closely associated clumps of trees from $>1$ to 207 trees (median 3.1 trees), and average percent of stand area $>6$ m from the nearest canopy ranging from 0% to 100% (median 5.1%). These ranges correspond well with past studies reporting density and spatial patterns of contemporary and historical active-fire reference stands in the Sierra Nevada, except this study observed greater total variation due to the much greater spatial extent of sampling. Within the montane forest zone, reference areas at middle elevations had lower density (86 vs. 121 trees $ha^{-1}$), basal area, (13.7 vs. 31 $m^2$ $ha^{-1}$), and mean clump size (2.7 vs. 4.0 trees) compared to lower- and higher-elevation reference areas, while ridgetops had lower density (101 vs. 115 trees $ha^{-1}$), basal area (19.6 vs. 24.1 $m^2$ $ha^{-1}$), and mean clump size (3.0 vs. 3.3 trees) and more open space (7.4% vs. 5.1%) than other landforms. Many of the relationships between physiography and reference structure were context-dependent, suggesting that management practices should create heterogeneous forest structure congruent with local climatic and topographic factors influencing stand conditions.

## 1. Introduction

Restoration of forest resilience – the ability of an ecosystem to maintain or quickly recover function after disturbance – is an important goal in contemporary forest management, especially in fire-dependent forests of the western United States (North et al., 2009; Churchill et al., 2013; Hessburg et al., 2013; DeRose and Long, 2014; Hessburg et al., 2015; Seidl et al., 2015; Johnstone et al., 2016; Stephens et al., 2016). Reference conditions describing characteristics of ecosystems that portray or embody desired functional outcomes can provide a quantifiable link between structure, composition, and desired function (Churchill et al., 2013). Reference conditions can serve as both waypoints to inform restoration targets (Kaufmann et al., 1998; Moore et al., 1999) and benchmarks for evaluating restoration progress (Christensen et al., 1996; Larson and Churchill, 2012). In either case, reference conditions use a desirable ecosystem as an example for relating function to measurable aspects of structure and composition.

Reference conditions in fire-dependent forests are often drawn from historical data, including recovered historical inventories (Leiburg, 1900; Langille, 1903; Munger, 1912; Collins et al., 2011; Hagmann et al., 2013; Lydersen et al., 2013; Hagmann et al., 2014) as well as reconstructed forest conditions (Fulé et al., 1997; Hessburg et al., 1999; Scholl and Taylor, 2010; Churchill et al., 2013; Barth et al., 2015; Schneider et al., 2015; Clyatt et al., 2016; Churchill et al., 2017). Historical references represent conditions that existed before Euro-American settlement when linkages between process and pattern remained

* Corresponding author.
E-mail address: jeronimo@uw.edu (S.M.A. Jeronimo).

https://doi.org/10.1016/j.foreco.2019.01.033
Received 15 October 2018; Received in revised form 19 January 2019; Accepted 22 January 2019

within the bounds of their evolutionary environment (Moore et al., 1999; Hessburg et al., 2005; Larson and Churchill, 2012), recognizing that Native American influences constituted a part of that environment (Vale, 2013). However, primary historical data suitable for defining reference conditions are rare and often limited in spatial extent and data quality (Stephens et al., 2015). Reconstructed forest conditions based on analysis of remnant structures (e.g., live trees, snags, and logs) can be quite uncertain for smaller trees, and the uncertainty increases as reconstructions reach farther back in time (Barth et al., 2015). Due to the amount of labor involved, reconstruction studies are also limited in their spatial extent. Thus, they are able to characterize stand-level structure adequately but may not capture variation across wide biophysical gradients within landscapes (Hessburg et al., 1999; Dickinson, 2014), an important aspect of restoration planning (Hessburg et al., 2015). Also, climates have been and are changing, limiting historical reference data because it describes forest conditions under a climate different than today (Millar and Woolfenden, 1999; Stephens et al., 2010; Heyerdahl et al., 2014; Hanberry et al., 2015; Hart et al., 2015; Johnstone et al., 2016).

Reference conditions can also be drawn from contemporary forests in areas where characteristic disturbance regimes have been maintained or reintroduced and modern anthropogenic disturbances like logging, mining, and grazing have been minimal (Taylor, 2010; Collins et al., 2016). In the western United States, fire is the primary process that structures dry forests (Brown et al., 2004; Hessburg et al., 2005), maintaining stands characterized by a fine-scale mosaic of tree clumps and canopy openings (Larson and Churchill, 2012; Churchill et al., 2013). Since the late 1960s, after about 60 years of fire suppression, forest managers in the Sierra Nevada region have been making a concerted effort to reintroduce frequent lower-severity fire to mixed-conifer forests, especially in National Parks (Parsons and Botti, 1996; van Wagtendonk, 2007). However, there has been no critical assessment of where fire regimes have begun to be restored in the Sierra Nevada nor how much of the region could be considered a reference condition. Defining contemporary reference conditions for the Sierra Nevada would supplement existing historical references in three important ways. First, contemporary measurements are precise with respect to sizes and locations of trees across the diameter distribution. Second, contemporary reference conditions inherently incorporate the effects of recent changes in climate. And third, remote sensing allows quantification of large reference landscapes.

The structural conditions associated with resilient forest ecosystems vary with fine-scale changes in topography and environment (Lydersen and North, 2012; Kane et al., 2015b; Churchill et al., 2017). Thus, a regional reference condition dataset should have a wide range of variation reflecting the diversity of physiographic and climatic conditions across the region. Reference conditions used for a given area should be drawn from an environmentally and climatically similar reference site to ensure that resilient conditions in one location will translate to another. This concept is derived from climate analogs (*sensu* Churchill et al., 2013), and we refer to it in a broadened sense as biophysical analogs.

Our objective was to identify and describe contemporary active-fire reference areas for different biophysical settings within the Sierra Nevada mixed-conifer zone to support planning, implementing, and monitoring restoration treatments. We sought to quantify how structure and spatial pattern vary with topography and climate. We conceptualized spatial pattern as a fine-scale mosaic of widely space individual trees, clumps of trees closely aggregated in space, and open space between tree crowns (Churchill et al., 2013).

Our research questions were:

(1) What is the geographic and environmental distribution of restored active-fire forest areas in the Sierra Nevada mixed-conifer zone?
(2) What are the ranges of variation in structure and spatial patterns across reference areas?

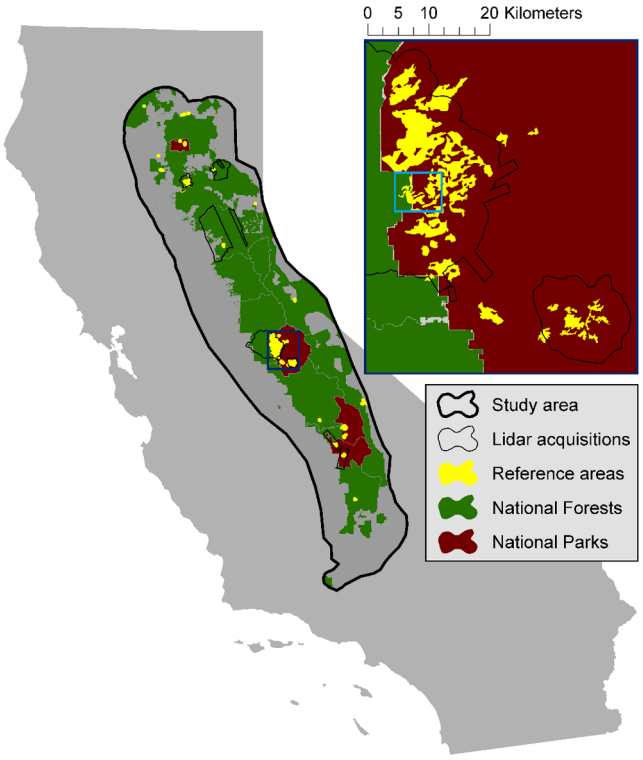


**Fig. 1.** Map of study area showing reference areas across the Sierra Nevada, federal ownership, and lidar acquisitions. Inset shows detail of area with high reference area density in western Yosemite. Light blue box indicates location shown in Fig. 3. (For interpretation of the references to colour in this figure legend, the reader is referred to the web version of this article.)

(3) How do density, tree clumping, and canopy opening patterns vary by topography and climate in reference areas?

## 2. Methods

### 2.1. Classifying the biophysical environment

#### 2.1.1. Climate classes

We began by defining climate classes across the Sierra Nevada (Fig. 1) to delineate the mixed-conifer zone and to provide the biophysical context for analyzing variation in reference condition structure.

We defined climate classes using the grain size of catchment basins. Catchment basins form ecologically relevant units (a connected watershed) that are familiar to forest managers and are operationally practical for mechanical (e.g., road building and yarding) and fire treatments (e.g., placement of fire line). We used basin data from the National Hydrography Dataset (EPA and USGS, 2018), with catchment sizes ranging from 7 to 1013 ha. We combined any catchments smaller than 100 ha with their immediate neighbors until a minimum size of 100 ha was reached; the smallest catchment after consolidation was 109.3 ha. For climate classification variables we focused on metrics integrating the biophysical conditions experienced by vegetation (Stephenson, 1998). Following the definition of climate analogs by Churchill et al. (2013), we selected actual evapotranspiration (AET) and climatic water deficit (Deficit) which are integrated measures of productivity and moisture stress, respectively (Lutz et al., 2010). We supplemented these with January minimum temperature ($T_{min}$), which can help to pinpoint limitations on regeneration and growth (Lutz et al., 2010; Dobrowski et al., 2013). We gathered annual AET, Deficit, and $T_{min}$ data averaged over the 1981–2010 period from the Basin Characterization Model dataset (Flint et al., 2013, 2014) at a 270 m pixel

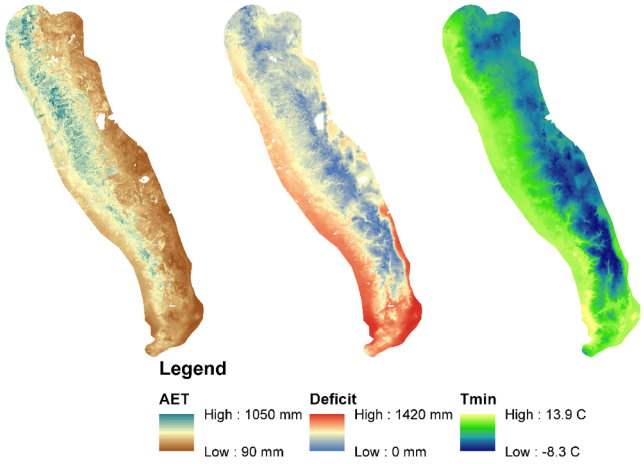


**Fig. 2.** Map of layers used to classify climate – annual actual evapotranspiration (AET), climatic water deficit (Deficit), and January minimum temperature ($T_{min}$) – across the study area. Data from Flint et al. (2014).

resolution. We calculated the 25$^{th}$ and 75$^{th}$ percentile from the values for each metric distributed throughout each catchment (Fig. 2).

We used the six resultant variables for each catchment (25$^{th}$ and 75$^{th}$ percentile values for each of AET, Deficit, and $T_{min}$) – normalized by global maxima – in a hierarchical classification with Euclidean distances and a complete linkage method, and implemented using the hclust function in R (R Core Team, 2016). We chose to use 20 classes by inspecting the dendrogram (Fig. A.1) and scree plot as well as by inspecting the classification results for cuts at 4, 8, 12, 16, 20, 24, 28, and 32 classes. We assigned descriptive names to each class based on inspection of the dendrogram and boxplots of class-wise distributions of AET, Deficit, and $T_{min}$ (Table 1, Fig. A.2).

We validated the climate classes by testing their ability to discriminate between forest composition using Sierra Nevada data from USFS Forest Inventory and Analysis (FIA) plots (Bechtold and Patterson, 2005). We selected 3217 plots that represent native forested communities using the following criteria: (1) minimum 10% forest cover, (2) natural stand origin, and (3) no artificial regeneration. We summarized composition on each plot by calculating proportions of live tree basal area by species and assigned each plot a climate class based on its publicly available fuzzed location (within 1.6 km of the true location).

We used PERMANOVA (McCune et al., 2002) to test whether composition varied by climate class. With the adonis function in the R package vegan (Oksanen et al., 2016), we compared proportionate live basal area by species across climate classes using the Bray-Curtis dissimilarity measure (Bray and Curtis, 1957) and assessed significance with 1000 permutations of climate class labels.

To provide a more specific idea of how composition varied by climate class we took two approaches to associating tree species with each climate class. First, we created lists for each class giving the species that are dominant by basal area on at least 5% of FIA plots, in decreasing order of dominance frequency.

Second, we performed an indicator species analysis (ISA) (McCune et al., 2002) to determine the most characteristic indicator species for each class. The ISA calculates indicator values (IVs) for each species in each class representing how faithful and how exclusive the species is to that class (McCune et al., 2002). We assessed significance of IVs using a permutation test, randomly shuffling the climate classes 1000 times. We assigned an indicator species to each class by taking the species with the highest IV that was also significant under the permutation test ($p < 0.05$). When two climate classes had the same indicator species we differentiated them by also considering the species with the second highest significant IV. For pairs of classes where the primary and secondary indicator species were both the same, we tested for differences in composition with PERMANOVA using the adonis function, Bray-Curtis dissimilarities, and 1000 permutations to assess significance.

We used the results of these two composition analyses to make associations between climate classes and the ecological zones and forest types defined by van Wagtendonk et al. (2018). We also associated the climate classes into five major groups: Foothills, Low Montane, Mid-Montane, Upper Montane, and High Sierra.

#### 2.1.2. Landscape management units

We subdivided catchments by topographic position to capture localized patterns of change in solar demand, soil depth, and water availability that can influence the biophysical environment and reference conditions at fine scales (Wiggins, 2017). We classified areas in terms of landscape management unit (LMU, *sensu* Underwood et al., 2010) using the Landscape Management Unit Tool version 2 (Boynton et al., 2015). This tool operates by classifying a digital elevation model (DEM) by topographic position. We used the simplified output from the tool and created the following classes based on a 30 m resolution DEM and default parameters: ridge, valley, SW slope (135–225° aspect), and NE slope (0–135° and 225–360° aspect). The resultant LMU sizes ranged from 0.1 to 56.6 ha and averaged 12.0 ha. We did not perform validation on the LMU classes since the nature of LMUs has already been described for California (Underwood et al., 2010; Lydersen and North, 2012; Wiggins, 2017).

### 2.2. Locating reference areas

We selected study areas in the Sierra Nevada mixed-conifer zone, where forests are dominated by a variable mix of ponderosa pine (*Pinus ponderosa*), Jeffrey pine (*P. jeffreyi*), sugar pine (*P. lambertiana*), white fir (*Abies concolor*), red fir (*A. magnifica*), and incense cedar (*Calocedrus decurrens*). This corresponds with the lower-montane and upper montane forest zones of van Wagtendonk et al. (2018) (Table 1). This zone is the center of most contemporary forest management in the Sierra Nevada and has a greater restoration need than other forest types due to its greater departure from characteristic fire return intervals (25–40 years greater departure than other Sierra Nevada forest zones) (Safford and Van de Water, 2014).

We defined reference areas across the Sierra Nevada based on management and fire history. We restricted the study to federal lands so that we had access to records of past management. This included all or part of 13 National Forests and three National Parks (Fig. 1). We created a raster layer at a 30 m resolution where pixel values were scored as integers from 0 to 5 representing how restored the fire regime of that pixel was (Fig. 3). One point was scored for each of the following criteria:

1. No records existed of past timber management (planting, harvest, thinning, etc.);
2. The pixel had experienced at least two fires in the last 60 years, so that a “regime” was beginning to be defined (Taylor, 2010; Lydersen and North, 2012; van Wagtendonk et al., 2012);
3. At least one of these fires occurred within the last 30 years, so that the results of reintroduced fire were still extant (Lydersen and North, 2012);
4. At least one of these fires had moderate severity effects on the pixels, because moderate severity fire kills more trees in lower canopy strata than low severity fire, thereby doing more work to return a fire-excluded stand to resilient conditions (Collins et al., 2011; Becker and Lutz, 2016); and
5. The pixel had not experienced high severity effects, because high amounts of mortality indicate low fire resistance (North et al., 2012; Stephens et al., 2013).

Timber management history data were retrieved from the Forest Service national geodata clearinghouse (USDA Forest Service, 2018), supplemented by manual inspection of aerial imagery for signs of

**Table 1**
Climate class characteristics in terms of climate variables, species composition, and forest type. Values shown here are descriptive; they are not the input values used for classification. AET = actual evapotranspiration, $T_{min}$ = annual minimum temperature. Species codes are given in Table A.1. Ecological zones, forest types, and historical fire return intervals are as defined by van Wagtendonk et al. (2018).

| Class | Reference area (area with lidar) (ha) | Median Values | | | | Species dominant by BA in at least 5% of plots | Indicator species |
|---|---|---|---|---|---|---|---|
| | | Elevation (m) | AET (mm) | Deficit (mm) | $T_{min}$ (° C) | | |
| Dry Foothills | – | 270 | 386 | 903 | 9.5 | QUDO, QUWI, PISA, QUCH | QUDO, QUWI |
| Hot Southern Foothills | – | 240 | 276 | 1145 | 9.8 | QUDO, QUWI, QUCH, AECA | QUDO, AECA |
| Warm Southern Foothills | – | 1280 | 241 | 1057 | 7.4 | QUDO, QUCH, QUWI, QUKE, PIMO | JUCA |
| Foothill Valleys | – | 390 | 553 | 640 | 9.4 | PIPO, PSME, LIDE, QUWI, QUDO | PSME, PIPO |
| Foothill-Low Montane Transition | – | 770 | 452 | 755 | 7.7 | QUCH, PIPO, QUWI, QUKE, QUDO, PSME, CADE | QUKE |
| Very Hot Low Montane | – | 770 | 545 | 617 | 7.6 | PSME, PIPO, QUKE, CADE | PSME, QUKE |
| Hot Low Montane | – | 1010 | 611 | 482 | 5.7 | PIPO, CADE, PSME, LIDE, QUKE, QUCH, ABCO | LIDE |
| South Sierra Low Montane | 933 (0) | 1740 | 160 | 927 | 3.9 | QUCH, PIMO, PIJE, ABCO, QUWI, QUKE, CADE | PIMO |
| Warm Dry Low Montane | 2121 (1505) | 1310 | 485 | 573 | 5.2 | PSME, ABCO, PIPO, QUKE, CADE, QUCH | PSME, QUKE |
| Warm Mesic Low Montane | 10,221 (9379) | 1670 | 376 | 620 | 3.5 | ABCO, CADE, PSME, PIPO, PILA, PIJE | CADE |
| Xeric Mid Montane | 1713 (1150) | 1470 | 229 | 756 | 1.9 | PIJE, JUOC, ABCO, CADE, QUCH, PIPO, PISA | PIJE, JUOC |
| Warm Mesic Mid Montane | 0 (0) | 1470 | 507 | 416 | 2.7 | ABCO, PSME, CADE, PIPO | ABCO, CADE |
| Cool Dry Mid Montane | 10,119 (7978) | 1810 | 359 | 517 | 1.5 | ABCO, ABMA, CADE, PSME, PIPO, PIJE | ABCO, ABMA |
| Xeric High Montane | 2566 (1695) | 1850 | 220 | 628 | 0.1 | PIJE, ABCO, JUOC, PIPO, ABMA, CADE | PIJE, JUOC |
| Cool Mesic High Montane | 524 (0) | 2170 | 443 | 321 | 0.0 | ABMA, ABCO, PICO, PIMO2, PIJE, TSME | ABMA, ABCO |
| Cool Dry High Montane | 2180 (1050) | 2110 | 298 | 465 | −0.8 | ABCO, ABMA, PICO, PIJE, PIPO | ABMA, PICO |
| Cold Dry High Montane | – | 2330 | 224 | 523 | −2 | PIJE, PICO, ABMA, ABCO, JUOC | PIJE, PICO |
| High Sierra | – | 2950 | 224 | 353 | −3.5 | PICO, PIAL, ABMA, PIBA | PICO |
| High Valleys and Meadows | – | 2880 | 379 | 155 | −3.8 | PIBA | PIBA |
| Subalpine | – | 3400 | 201 | 252 | −5.1 | PIAL, PICO, PIBA, TSME | PIAL |

| Class | Ecological zone | Common forest type(s) | Historical fire return interval |
|---|---|---|---|
| Dry Foothills | Foothill shrubland and woodland | QUDO woodland, PISA-QUWI woodland | Short |
| Hot Southern Foothills | Foothill shrubland and woodland | QUDO woodland, mixed hardwood woodland | Short |
| Warm Southern Foothills | Foothill shrubland and woodland | QUDO woodland, mixed hardwood woodland | Short-Medium |
| Foothill Valleys | Foothill shrubland and woodland/Lower-montane forest transition zone | QUDO woodland, PISA-QUWI woodland, riparian forest | Medium |
| Foothill-Low Montane Transition | Foothill shrubland and woodland/Lower-montane forest transition zone | Mixed hardwood woodland, QUDO woodland, mixed evergreen | Short-Medium |
| Very Hot Low Montane | Lower-montane forest | QUKE-PIPO-ABCO-PSME forest, mixed evergreen | Short |
| Hot Low Montane | Lower-montane forest | QUKE-PIPO-ABCO-PSME forest, mixed evergreen | Short-Medium |
| South Sierra Low Montane | Lower-montane forest | QUKE-PIPO-ABCO-PSME forest, mixed conifer | Short |
| Warm Dry Low Montane | Lower-montane forest | Mixed evergreen, mixed conifer | Short |
| Warm Mesic Low Montane | Lower-montane forest | Mixed conifer | Short |
| Xeric Mid Montane | Lower-montane forest/Upper montane forest transition zone | PIJE woodland, JUOC woodland, mixed evergreen | Short |
| Warm Mesic Mid Montane | Lower-montane forest/Upper montane forest transition zone | Mixed conifer | Short |
| Cool Dry Mid Montane | Lower-montane forest/Upper montane forest transition zone | Mixed conifer, PIJE woodland | Short-Medium |
| Xeric High Montane | Upper montane forest | PIJE woodland, mixed conifer, JUOC woodland | Medium |
| Cool Mesic High Montane | Upper montane forest | ABMA forest, PIMO2 forest, PIJE woodland | Medium |
| Cool Dry High Montane | Upper montane forest | ABMA forest, PICO forest, PIJE woodland | Medium-Long |
| Cold Dry High Montane | Upper montane forest | PIJE woodland, PICO forest, ABMA forest, JUOC woodland | Medium-Long |
| High Sierra | Upper montane forest/Subalpine forest transition zone | PICO forest, PIAL woodland, ABMA forest, PIBA woodland | Long |
| High Valleys and Meadows | Subalpine forest | PIBA woodland | Long |
| Subalpine | Subalpine forest | PIAL woodland, PICO forest, PIBA woodland, TSME forest | Long |

mechanical treatment in potential reference areas. Low-intensity historical logging may have been missed in this procedure. We did not consider management history for National Parks aside from prescribed burning, since mechanical treatments have seldom been used in park management. Fire history was drawn from the FRAP fire atlas (Cal Fire, 2018) for years 1957–1983 and Monitoring Trends in Burn Severity (Eidenshink et al., 2007) for years 1984–2014. The Cal Fire (2018) data did not include spatially explicit burn severities, so we treated all management ignitions as low severity fires throughout. Fires started by lightning and accidental human ignition were assumed to be low severity when they were small (< 400 ha) and successfully suppressed within a 3 days. Larger fire areas from 1957 to 1983 with unknown severity were excluded from the analysis.

Using the defined raster layer, we drew polygons around areas with high scores (at least four, mostly five), following natural boundaries of fire history and topography to separate areas (Fig. 3). We enforced the following criteria for each area:

1. Patch size was at least 100 ha, to provide a meaningful sample of fire effects within each one;
2. Any high-severity patches incorporated into the reference area were no larger than 10 ha, since the majority of high-severity patches

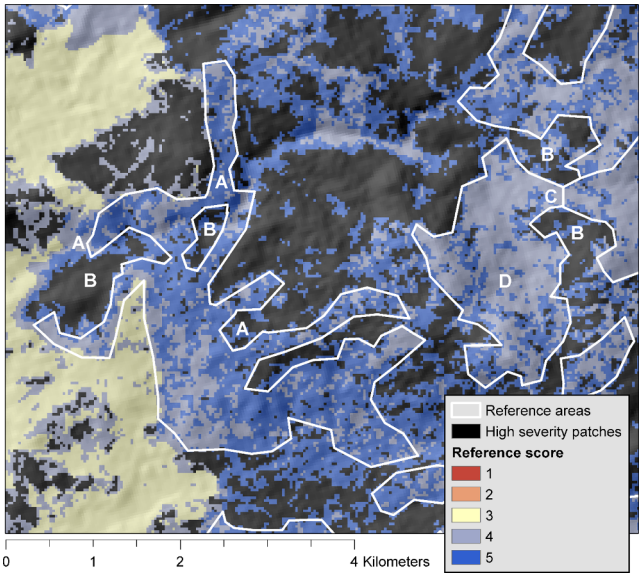


**Fig. 3.** Illustration of reference patch delineation, showing some key elements of the manual delineation methods. The background reference score (Landsat pixel size of 30 m) ranges from one to five depending on fire history (section 2.2). Constraints applied in patch delineation: (A) Stringers were cut off at a 100 m width threshold. (B) High-severity patches greater than 10 ha in size were excluded. This resulted in "donut holes" when the 100 m width threshold allowed. (C) Contiguous patches were split apart on catchment divides (pictured) and fire perimeters. (D) Areas scoring mostly five were favored but areas scoring mostly four were allowed when the only criterion not met was "at least one moderate severity fire" and the number of fires was greater than two.

found historically were no more than a few hectares in size (Kilgore, 1973; Skinner and Chang, 1996; Keeley and Stephenson, 2000);

3. No more than 10% of the polygon had burned at high severity, which is near the high end of the range of variation in historical high severity proportions (Mallek et al., 2013 and references therein; Stephens et al., 2015);
4. The average number of fires in the polygon was ≥ 2, to ensure that the area has, on the whole, experienced multiple fires; and
5. The average number of recent fires (< 30 yr. old) in the polygon was ≥ 1, to ensure that the area has, on the whole, burned recently.

These criteria ensured that polygons represent patches with a variety of patterns, mainly characterized by pixels with a score of five (Fig. 4). The criteria allowed for flexibility in several ways. First, even though high-severity pixels were not favored in the pixel criteria, we recognized that some amount of high severity fire is expected to occur in reference areas (Collins and Stephens, 2010; Mallek et al., 2013) and so some high-severity patches were included. We chose to make the limits for high severity inclusion within these areas liberal relative to published historical conditions because (1) studies capturing historical conditions likely missed some of the largest patches and, (2) these reference stands have had several fires recently but are still recovering from decades of fire suppression, so we did not expect them to fully match historical conditions. The criteria also allowed for unburned patches to be incorporated within the matrix of burned lands. This is intentional, since unburned refugia are critical elements of resilience in post-fire landscapes (Kolden et al., 2015; Meddens et al., 2018; Meigs and Krawchuk, 2018). In contrast, we did not allow any mechanical treatment activity within the reference areas.

We visited 11 of the 85 identified reference areas, focusing on northwestern Yosemite. We walked through the areas in an informal survey guided by aerial photos and the lidar canopy models with the goal of seeing as many different kinds of conditions as possible. We collected notes and photographs characterizing forest structure over a total path length of about 200 km. We used the qualitative data collected in these visits to improve our interpretation of fire history data and modified reference area boundaries in light of what we learned. Specifically, we redrew boundaries to more closely follow topographic features, we became stricter with excluding high severity areas, and we decided to allow patches that had only burned at low severity when they had burned three or more times.

### 2.3. Quantifying reference area structure

We used lidar data to characterize the forest structure of the reference areas and provide a set of quantitative reference conditions. Lidar data provides measurements of structure at a resolution of several data points per square meter across areas tens to hundreds of thousands of hectares in size, and so allowed us to quantify structural variation across entire reference areas. We characterized structure using lidar-identified tree-approximate objects (TAOs) (North et al., 2017; Jeronimo et al., 2018). TAOs are an ecologically meaningful unit of measurement representing a canopy tree that was detected by the lidar along with subordinate trees that cannot be individually resolved. The canopy tree may be an individual with no subordinates or may be associated with a small number of understory trees (mean 1.5 [sd 1.2] undetected trees per TAO; S. Jeronimo, *unpublished data*). Using TAOs allows for a consistent unit of analysis even while tree detection accuracy changes with forest structure (Jeronimo et al., 2018). Since large trees, which are more visible to lidar, dominate basal area and spatial heterogeneity (Lutz et al., 2012, 2013, 2018), directly measuring patterns of TAOs maintains much of the useful information that would be gathered in a traditional tree-based survey. By necessity, this portion of the analysis was limited to areas with available lidar data (Fig. 1; Table 2). This included 76% of the identified reference areas, or 23,088 ha.

Across each lidar acquisition area we created ground-normalized canopy height models using a 0.75 m resolution and a 3 × 3 pixel smoothing window (Jeronimo et al., 2018) and segmented the canopy height model into TAOs using the TreeSeg tool in the FUSION Lidar Toolkit (McGaughey, 2018). The TreeSeg tool associates each TAO with a location and a height. We additionally modeled dbh for each TAO using regressions developed from the 3217 FIA plots described above. We used the following regression model form:

$$\text{dbh} = b_0 \text{height}^{b_1}, \quad (1)$$

fitting a separate set of coefficients for each climate class (Table A.2).

We split reference areas into polygons by LMU, and for each polygon calculated summary metrics quantifying conditions in terms of TAO size distributions, stocking, and spatial pattern. We did not attempt to separate TAOs dominated by a live tree from TAOs dominated by a snag. Size distributions were quantified in terms of modeled dbh distributions. Stocking was quantified by TAO density and basal area based on modeled dbh. Spatial pattern metrics followed the Individuals, Clumps, and Openings method (ICO) (Churchill et al., 2013). TAOs were considered members of the same clump if their high points were within 6 m of one another, and TAOs with no neighbors within 6 m were considered individuals. This limiting distance was chosen to represent the average crown width of a mature conifer and was validated using plot data from Yosemite ($n$ = 97 trees, data not shown). Clump size distributions were reported as proportions of TAOs in clumps of different sizes: individuals, small clumps (2–4 TAOs), medium clumps (5–9 TAOs), large clumps (10–14 TAOs), super clumps (15–30 TAOs), and mega clumps (> 30 TAOs). Any area with no vegetation taller than 2 m in the canopy height model was considered open space. We created open space distributions to describe the amount of area at varying distances from the nearest canopy: 0–10 m in 2 m bins, 10–20 m, and > 20 m (Churchill et al., 2017). We delineated canopy gaps with methods from Lydersen et al. (2013), which uses image morphology


**Fig. 4.** Photos exemplifying conditions in reference areas. (a) shows a hillslope view exhibiting a complex patch mosaic. (b), (c), and (d) show open, fire-resistant conditions with scattered large trees and very little understory. (e) and (f) show sites that have burned fewer times or at lower severity, where stem density appears high but most small trees are dead and surface fuel loads are low.

operations to identify gaps at least 60 $m^2$ in size and cut off long meandering gaps at ecologically relevant thresholds. Gaps were summarized in terms of gap density and gap size distributions. Clumps, open space, and gaps were all quantified across entire reference areas before being subdivided by LMU to avoid edge effects.

**Table 2**
Lidar acquisitions used in this study and their key technical specifications. Vendor abbreviations: WSI = Watershed Sciences, Inc. (today Quantum Spatial), NCALM = National Center for Airborne Laser Mapping, CIS = Carnegie Institution for Science. CAO = Carnegie Airborne Observatory (Asner et al., 2007).

| Acquisition | Illilouette Basin | Rim Fire | Sequoia National Park | Storrie Fire | Moonlight Fire | Tahoe National Forest |
|---|---|---|---|---|---|---|
| Mo./yr. acquired | Aug. 2011 | Nov. 2013 | Aug. 2015 | Aug. 2009 | Aug. 2013 | Jun. 2013 |
| Collected by | WSI | NCALM | CIS | WSI | WSI | NCALM |
| Instrument | Dual Leica ALS50 ii | Optech Gemini ALTM | CAO | Dual Leica ALS50 ii | Dual Leica ALS50 ii | Optech Gemini ALTM |
| Max. returns per pulse | 4 | 4 | 4 | 4 | 4 | 4 |
| Average pulse density (# $m^{-2}$) | 12 | 12 | 14 | 7 | 11 | 8.5 |
| Laser pulse frequency (kHz) | 83 | 125 | 100 | 90 | 90 | 100 |
| Field of view (°) | ± 14 | ± 14 | ± 17 | ± 14 | ± 14 | ± 18 |

### 2.4. Differences in reference structure across biophysical environments

To assess how structure of reference areas changes across different biophysical environments we tested for differences in forest structure and pattern between climate and LMU classes, including an interaction term, using analysis of variance (ANOVA) and structural indices. We used data from the six climate classes that had at least 100 ha of reference areas with lidar coverage (Warm Dry Low Montane, Warm Mesic Low Montane, Xeric Mid Montane, Cool Dry Mid Montane, Xeric High Montane, and Cold Dry High Montane). The structure and pattern indices were TAO density, TAO basal area, mean clump size, and proportion of open space > 6 m from the nearest canopy. These metrics are a good summary of stocking and pattern (Churchill et al., 2013). The indices were calculated based on LMUs within each reference area. We confirmed that the distributions of the indices met the assumptions of ANOVA, which required log-transforming the clump and opening indices. We then tested for significant differences between climate and LMU classes for each of these metrics in separate univariate two-way ANOVAs. For any tests that gave significant results we used a Tukey HSD post-hoc test to find significant differences between pairs of classes.

## 3. Results

### 3.1. Climate classes

The 20 climate classes identified across the Sierra Nevada were distinctly different in terms of AET, Deficit, $T_{min}$, and species composition (Fig. A.2). The warmest, driest class, Dry Foothills, had a median AET of 386 mm (range 229–856 mm, mean 396 mm), a median Deficit of 903 mm (range 317–1202 mm, mean 893 mm), and a median $T_{min}$ of 9.5 °C (range 2.1–12.5 °C, mean 9.4 °C). In contrast, the coldest, wettest class, Subalpine, had a similar median AET of 379 mm (range 100–483 mm, mean 207 mm), a much lower median Deficit of 155 mm (range 12–767, mean 255 mm), and a median $T_{min}$ of −3.8 °C (range –8.3 to 0.9 °C, mean –5.2 °C) (Table 1). Five classes fell into the Foothills category, five were Low Montane, three were Mid-Montane, four were Upper Montane, and three were High Sierra. Geographically, climate class groupings followed two major gradients: latitude and elevation. A noticeable break in classification occurred around 38°N latitude, with some higher-Deficit classes introduced south of that line. The elevation gradient is clear, and is expressed in roughly parallel bands running north-south along the range (Fig. 5).

Composition of FIA plots was different among climate classes ($p < 0.01$). Classes in the Foothills group were dominated by oaks (*Quercus* spp.) and gray pine (*Pinus sabiniana*), with California buckeye (*Aesculus californica*) and single-leaf pinyon (*P. monophylla*) in the Southern Foothills. Ponderosa pine, Douglas-fir (*Pseudotsuga menziesii*), and tanoak (*Lithocarpus densiflorus*) occurred in Foothill Valleys and incense-cedar additionally occurred in the Foothills-Low Montane Transition zone. Low Montane classes were dominated by Douglas-fir, white fir, sugar pine, incense cedar, and ponderosa pine, but red fir was notably absent. California black oak (*Q. kelloggii*) was also common and canyon live oak (*Q. chrysolepis*) was present. Sugar pine was most dominant in the Warm Mesic Low Montane class. Mid-Montane classes had a similar species assemblage but also included red fir, and Jeffrey pine was dominant in the Xeric Mid Montane class. High Montane classes were dominated by red fir, Jeffrey pine, and white fir, with some of the other pines still present. Lastly, the High Sierra group was dominated by high-altitude pines (*P. contorta*, *P. albicaulis*, and *P. balfouriana*) with some red fir and mountain hemlock (*Tsuga mertensiana*) (Table 1).

The indicator species analysis (ISA) yielded significant results for all climate classes. Within the Montane classes Douglas-fir and California black oak were indicators for warmer, drier classes (high AET and high Deficit) while incense cedar indicated cooler classes (lower $T_{min}$).

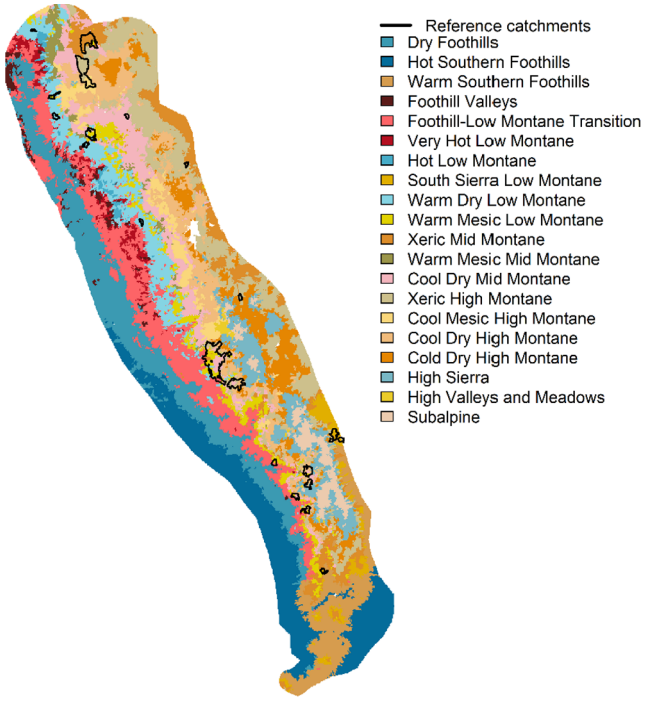


**Fig. 5.** Map of climate classes. Catchments containing at least one reference area indicated to illustrate the environmental distribution of reference areas.

Edaphically xeric classes (low AET with high Deficit) were indicated by Jeffrey pine and western juniper (*Juniperus occidentalis*). Red fir and lodgepole pine (*P. contorta*) indicated classes with $T_{min}$ values at or below 0 °C (Table 1).

There were two cases when pairs of classes shared the same primary and secondary indicator species. The Very Hot Low Montane class and the Warm Dry Low Montane class both had Douglas-fir and California black oak as indicators, and the Xeric Mid Montane and Xeric High Montane classes shared Jeffrey pine and western juniper. In both cases PERMANOVA tests with pairwise contrasts showed significant differences in FIA plot composition ($p < 0.01$).

### 3.2. Reference areas

We identified a total of 30,377 ha of reference areas across the Sierra Nevada mixed-conifer zone (Table 1). Median contiguous patch size was 260 ha and the maximum was 5500 ha. Reference areas were distributed across the latitudinal and altitudinal ranges of our study area, mostly on the west slope of the Sierra Nevada (Fig. 1). By far the majority of reference area was in the central and southern Sierra (25,663 ha), concentrated in Yosemite National Park (19,990 ha) and Sequoia-Kings Canyon National Park (3927 ha), along with 1380 ha on the Sierra, Sequoia, and Inyo National Forests. The majority of reference areas in the northern Sierra were on the Plumas and Lassen National Forests (3532 ha) and Lassen National Park (701 ha).

### 3.3. Reference conditions

The envelope of reference area structure was broad and variable (Figs. 4, 6). TAO density varied from 6 to 320 TAOs $ha^{-1}$ distributed widely across diameter classes (Fig. 6b). Typical LMUs had up to 42.9 TAOs $ha^{-1}$ < 20 cm dbh, up to 29.2 TAOs $ha^{-1}$ 20–40 cm dbh, up to 26.0 TAOs $ha^{-1}$ 40–60 cm, up to 21.6 TAOs $ha^{-1}$ 60–80 cm, up to 15.3 TAOs $ha^{-1}$ 80–100 cm, and up to 7.4 TAOs $ha^{-1}$ 100–120 cm dbh (all values given are 75$^{th}$ percentile values) (Fig. 6a). Overall density was normally distributed (Fig. 6b) with a mean of 111 TAOs $ha^{-1}$ and a standard deviation of 40 TAOs $ha^{-1}$. Basal area was distributed with a

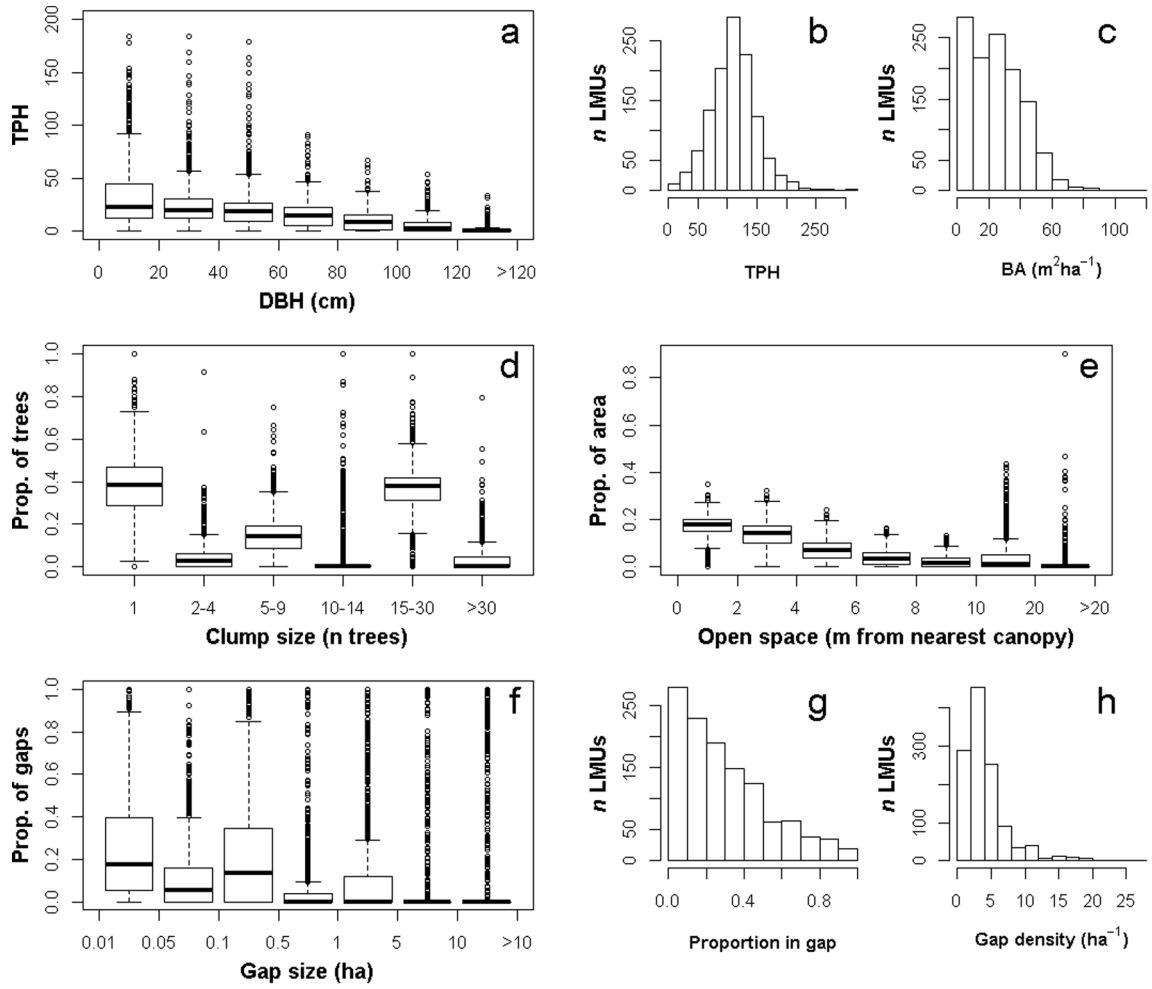


**Fig. 6.** Ranges of variation in reference condition structure across all reference areas with available lidar data. Each data point represents one landscape management unit. TPH = TAOs per hectare, DBH = diameter at breast height, BA = basal area. Horizontal axes for panels a, e, and f show break points between bins.

mode at 25 $m^2$ $ha^{-1}$ (standard deviation 17 $m^2$ $ha^{-1}$) and a right skew. The majority of LMUs had less than 10 $m^2$ $ha^{-1}$ of basal area, but only five percent had less than 2 $m^2$ $ha^{-1}$ (Fig. 6c).

Spatial patterns of TAOs in reference areas had some consistent patterns of variation. TAOs were most commonly arranged as individuals with no close neighbors and in clumps of 15–30 (both median 38% of TAOs per LMU). LMUs with many clumps of 2–14 or > 30 TAOs were less common (Fig. 6d). Between 25% and 40% of stand area was usually situated in openings < 4 m from the nearest canopy, whereas less than 15% was usually > 6 m from the nearest canopy. However, as is evident in the basal area distribution, some LMUs were very open and it was not uncommon for 10–20% of the LMU area to be located > 10 m from the nearest canopy (Fig. 6e). Delineated gaps at least 12 m in diameter were present on 94% of LMUs, usually representing < 50% of LMU area. On most LMUs the majority of gaps were under 0.5 ha in size (median 72%), with 25% under 0.05 ha (Fig. 6f). However, larger gaps were often present including commonly up to 13% of gaps in the 1–5 ha size class, and 94% of total gap area across reference areas was accounted for by gaps ≥ 1 ha. Most LMUs had 0–10% of area in gaps (Fig. 6g) at a density of 2–5 gaps $ha^{-1}$, and up to 8 gaps $ha^{-1}$ was common (Fig. 6h). The highest observed gap density was 26 $ha^{-1}$.

### 3.4. Variation in reference structure across biophysical environments

All of the stocking and spatial pattern indices we tested varied significantly by climate class and LMU. Density and mean clump size also had significant climate class-LMU interaction terms (Fig. 7). Of the six climate classes analyzed the lowest- and highest-elevation classes had the highest densities (median 121 TAOs $ha^{-1}$), following a roughly U-shaped distribution across the elevation gradient. The Xeric Mid Montane class had significantly lower density than any other class (median 86 TAOs $ha^{-1}$). Density was also significantly lower on ridges compared to valleys, but the absolute difference was not large (medians 101 vs. 115 TAOs $ha^{-1}$). Ridges and valleys diverged from the general U-shaped distribution in the highest elevation class, Cold Dry High Montane, where densities were almost as low as for the Xeric Mid Montane class (Fig. 7). Basal area followed density in its response to topography (slightly lower on ridges), but its relationship with climate was more complex. The two edaphically xeric classes had lower basal area (median 3.7 and 22 $m^2$ $ha^{-1}$) as did the Warm Mesic Low Montane class (median 13.7 $m^2$ $ha^{-1}$). However, the Cool Dry Mid Montane class, which had relatively low density, had the highest basal area (median 31 $m^2$ $ha^{-1}$). There was no significant climate class-LMU interaction for basal area.

Mean clump size was indistinguishable among five of the six tested climate classes (Fig. 7). The Cool Dry Mid Montane class had a lower mean clump size than the rest (median 2.7 vs. 4.0 trees). Mean clump size differed between ridges (median 3.0 trees) and other landforms (median 3.3 trees). More pronounced was the interactive effect of climate class and LMU on mean clump size. Clump sizes were larger in valleys compared to other landforms in the Warm Dry Low Montane, Xeric Mid Montane, and Xeric High Montane climate classes (Fig. 7). Southwest-facing slopes also had higher mean clump sizes in the Xeric

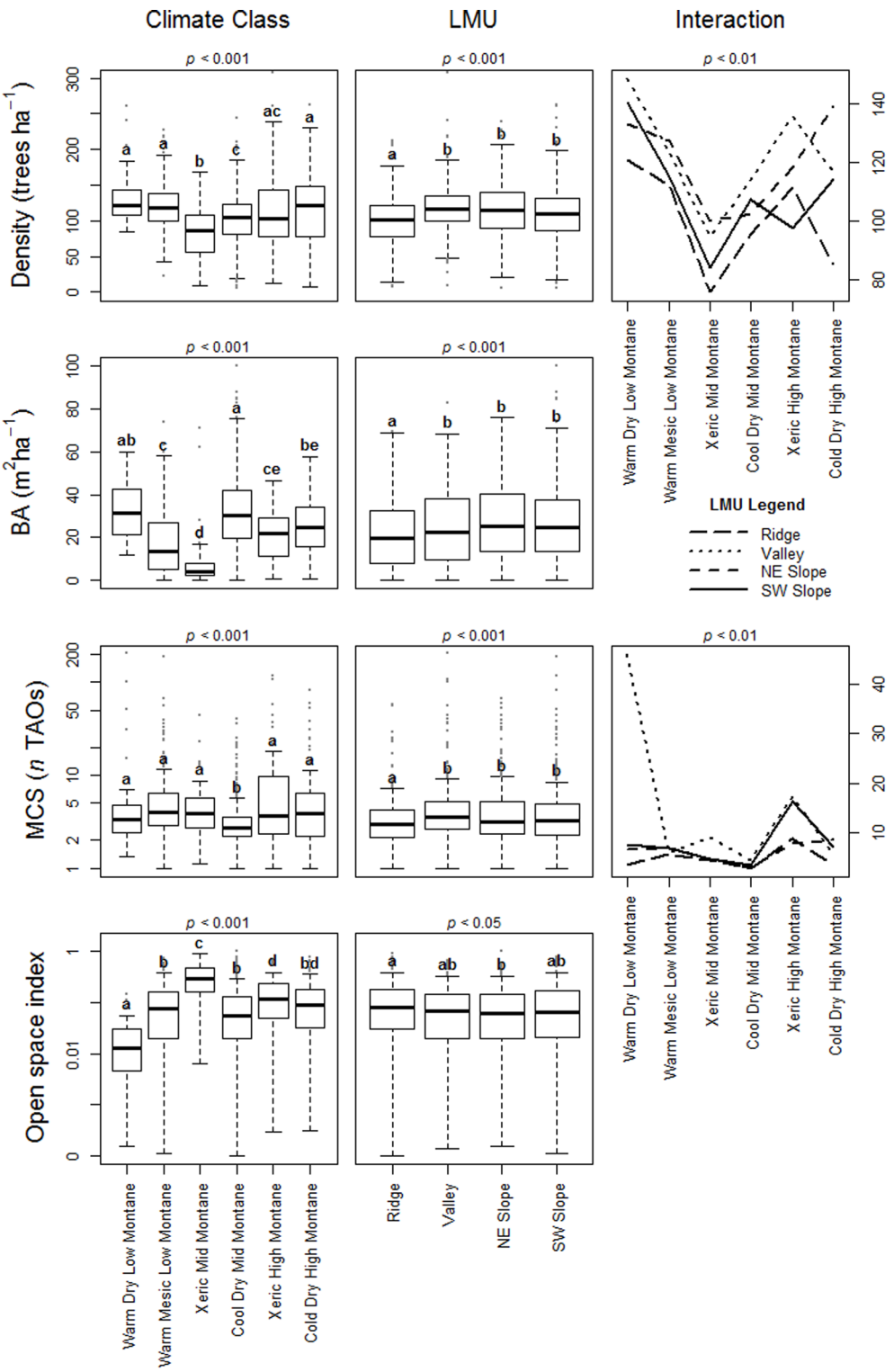


**Fig. 7.** Structure and pattern indices varying by climate class and landscape management unit (LMU). Interaction terms are shown where significant. Letters above box plots indicate statistically distinct groupings based on Tukey tests. Open space index refers to the proportion of area > 6 m from the nearest canopy. BA = basal area, MCS = mean clump size, TAO = tree-approximate object.

High Montane climate class. The open space index, measuring the proportion of stand area greater than 6 m from the nearest canopy edge, varied across climate classes and LMUs almost as a mirror image of basal area when plotted on a log scale (Fig. 7). The open space index was lowest in the Warm Dry Low Montane class (median 0.01) and highest in the Xeric Mid Montane class (median 0.29). Open space was higher on ridges (median 0.074) and lower on NE-facing slopes (median 0.046), while valleys and SW slopes were transitional (median 0.056).

## 4. Discussion

We found that contemporary fire-dependent forests, often used to inform restoration targets, vary by climate and topographic position, producing an array of structural conditions that are highly variable at

landscape scales. Our results reaffirm the importance of managing for wide and flexible ranges of variation at multiple scales rather than managing for one specific condition at any one scale (Larson and Churchill, 2012; Hessburg et al., 2015; Collins et al., 2016). Given the complex relationship between environmental setting and reference condition structure, it is valuable to use the most biophysically analogous data available for evaluating departure from reference conditions (Churchill et al., 2013). We found that climate classes at coarse scales and LMUs at fine scales provided a meaningful biophysical template for forest structure and spatial pattern. Using this framework, management objectives for a departed landscape could be defined to produce a range of stand structures congruent with climatic and physiographic factors that may improve forest resilience to increasing severity and frequency of fire and drought stresses.

### 4.1. Geographic and environmental distribution of reference areas

The geographic distribution of reference areas was most obviously due to management practices associated with different land ownerships. We required that reference areas had no history of active forest management such as planting, thinning, or logging. Timber management has been widespread across National Forests of the Sierra Nevada since the early 1900s (Laudenslayer and Darr, 1990), but has generally not occurred in the National Parks which were protected from most resource extraction starting in 1890 (Yosemite and Sequoia-Kings Canyon) and 1907 (Lassen) (Parsons and van Wagtendonk, 1996). Logging that did occur before the parks were protected was mostly opportunistic and small-scale (Laudenslayer and Darr, 1990). Second, fire policy has been very different between National Forests versus National Parks in the Sierra Nevada, especially since the early 1970s when the parks began phasing out full suppression policies and adopting instead active prescribed fire and managed wildfire programs (Parsons and Botti, 1996; van Wagtendonk, 2007; van Wagtendonk and Lutz, 2007). In contrast, National Forests started using prescribed burning more recently and have adopted managed wildfire primarily in designated wilderness (Stephens and Ruth, 2005). This in large part accounts for the fact that 81% of the reference area in the Sierra Nevada mixed-conifer zone is in National Parks, even while the parks represent less than 13% of the federal land base in the Sierra Nevada.

Some part of the distribution of reference areas can also be attributed to environmental conditions, in particular, lightning strikes. Lightning ignitions are an important environmental factor in Sierra Nevada fire regimes, since essentially all of the montane forest is dry enough to burn during the annual summer drought (Lutz et al., 2009). Lightning strike density varies with elevation across the Sierra, peaking in the 1800–2400 m elevation band (van Wagtendonk, 1994; van Wagtendonk and Cayan, 2008). This may explain why there were no reference areas in the two lowest-altitude montane climate classes (Very Hot Low Montane, Hot Low Montane). The elevation band that these classes primarily occupy, 600–1200 m, receives less than half as many lightning strikes of any of the other montane classes, and less than a quarter as many strikes as the three highest-elevation montane classes (van Wagtendonk and Cayan, 2008). Another explanation may be the tendency of forests in this elevation band to burn in human-caused fires with large high-severity patches.

A final factor that influenced the distribution of reference areas was the 2013 Rim fire. The Rim fire burned 31,519 ha of western Yosemite (Lydersen et al., 2014), reburning a series of fires from the 1980s to 2000s that had substantial lower-severity components. This initial series of fires primed western Yosemite for a subsequent lower-severity burn. Although the Rim fire burned at high severity on the adjacent Stanislaus National Forest, severity in Yosemite was much more mixed in part because of the previous fire history (Lydersen et al., 2014; Kane et al., 2015a; Lydersen et al., 2017). Over half of the reference areas in Yosemite only met our criteria after being burned by the Rim fire.

### 4.2. Ranges of variation in reference stand structure and pattern

The ranges of variation in density that we measured in reference areas generally matched ranges reported by past studies quantifying active-fire Sierra Nevada forest structure. For example, several reconstructed and historical datasets report mean densities ranging from 60 to 314 TAOs $ha^{-1}$, with total density ranges from 16 to 650 TAOs $ha^{-1}$ (minimum dbh values varied from 5 to 15.2 cm) (North et al., 2007; Scholl and Taylor, 2010; Collins et al., 2011; Van de Water and North, 2011; Knapp et al., 2013; Barth et al., 2015; Stephens et al., 2015). This matches well with our measured mean density of 111 TAOs $ha^{-1}$ (range 6–320), even when considering that each TAO may represent both the identified overstory tree and up to several subordinate trees. These same studies report mean basal area between 21 and 54 $m^2$ $ha^{-1}$ with a range of 0.3–89 $m^2$ $ha^{-1}$, compared to our mean basal area of 25 $m^2$ $ha^{-1}$ (range 0.01–113). This alignment indicates that the reference areas we identified exhibit some of the key structural features associated with historically resilient stands, namely, lower densities than contemporary fire-suppressed forests and dominance by large trees (North et al., 2009; Stephens et al., 2015; Safford and Stevens, 2017). However, dominance by large trees was not observed in every reference area. In particular, small old trees (often 10–20 cm dbh observed during field visits) dominated the Xeric Mid-Montane climate class, which is characterized by shallow, gravelly soils with very sparse forest cover and stringers of denser cover in patches of convergent topography.

In contrast, correspondence between our measurements of spatial pattern and reported measurements for historical Sierra Nevada forests was mixed. We are aware of only one study using spatially-explicit data to describe historical spatial patterns in the Sierra Nevada: Lydersen et al. (2013) used 1929 stem map data from the “Methods of Cutting” experiment on the Stanislaus-Tuolumne Experimental Forest to quantify tree clumps and canopy opening patterns. Our measurements of TAO clumps did not directly align with their measurements of tree clumps. Specifically, we measured a higher proportion of individuals (38% vs. 5.6%) and a lower proportion of small clumps of 2–4 trees/TAOs (4.2% vs. 13.4%). This is probably because many TAOs counted as individuals actually represent two or three trees. In this sense our data and the data from Lydersen et al. (2013) are not directly comparable. However, measurements of open space do not rely on tree counts and so can be directly compared. Our average measurements were similar to the Methods of Cutting plots. Lydersen et al. (2013) found 40% of plot area was in open space $< 3$ m from the nearest canopy compared to our finding of 25–40% within 4 m. The Methods of Cutting plots averaged 5.2 delineated gaps $ha^{-1}$ compared to our 4.1 $ha^{-1}$, and the distributions of gap sizes were also comparable. We additionally identified many large gaps ($> 10$ ha) that were not possible to detect with the 4 ha plots used by Lydersen et al. (2013).

Contemporary measurements of spatial pattern in the active-fire Sierra San Pedro Martir in northern Baja California, Mexico provide another point of reference. Fry et al. (2014) found that 10–14% of trees in Jeffrey pine-mixed conifer stands were individuals with no close neighbors, while 20–25% of trees were in small clumps and 18–24% of trees were in medium clumps of 5–9 trees. These proportions represent a somewhat less clumped stand than the Lydersen et al. (2013) data (more individuals and small clumps, fewer large clumps), but compare to our findings similarly. That is, we found higher proportions of individuals and lower proportions of small clumps overall.

### 4.3. Variation in reference structure across biophysical environments

Patterns of variation in active-fire forest structure are very complex, driven by multiple interactions between fire, topography, and moisture (Kane et al., 2013, 2015a; Collins et al., 2016). Some of this variation can be explained by elevation, water balance, and topographic position. For example, Collins et al. (2015) found that elevation and AET strongly differentiated between different classes of tree size and stand basal

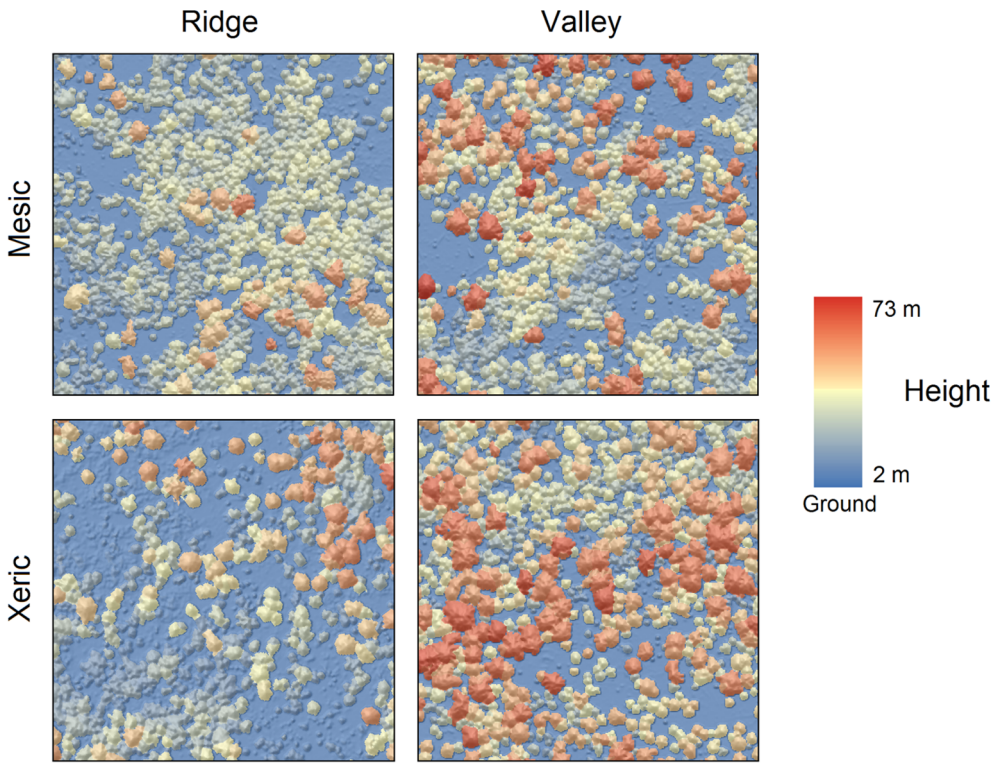


**Fig. 8.** Example illustrating context-dependent relationships of climate and landform driving structure and pattern in reference areas, as is quantitatively shown in Fig. 7. In mesic conditions, density and spatial patterns are similar between ridges and valleys; only the sizes of trees differ. In xeric conditions trees are still larger in valleys than on ridges, but density and mean clump size are also higher in valleys.

area. Kane et al. (2015b) found that AET and Deficit, along with slope and topographic position, were good predictors of canopy cover and tree height in twice-burned stands. Lydersen and North (2012) found gradients of tree size and density associated with slope position, which differentiated between structural conditions better than aspect did. However, there was residual variation around these patterns in all cases. Our results suggest that the way the biophysical environment drives structure in active-fire landscapes is context-dependent, which may partially account for high amounts of unexplained variation in earlier research. This agrees with findings of Abella et al. (2015) from the Spring Mountains of Nevada. Here we provide examples illustrating the complex context dependency in relationships between the biophysical environment and structure (Fig. 8).

We found that ridgetops had lower density, lower basal area, smaller tree clumps, and more open space than other landforms (Fig. 7). This matches descriptions by Lydersen and North (2012), who suggest that ridges uniquely combine lower productivity with more severe fire effects (i.e., more fire mortality) to result in a fundamentally different growing environment than other landforms. However, climate conditions can alter or enhance this relationship. For instance, the basic relationship between landform and density is reversed in the Xeric High Montane climate class, where ridges are similar to NE slopes while SW slopes have the lowest density (Fig. 7). One possible explanation is that this climate class is characterized by shallow, rocky soils throughout, so ridgetop soil conditions are not very different from other landforms. This normalization of landform effects may allow the (usually less important) effect of aspect on insolation to be expressed in the form of reduced density on SW slopes. In contrast, the relationship between landform and density is enhanced in the Cold Dry High Montane class, where ridgetop density was lower than density on other landforms by a much greater margin than in any other climate class (Fig. 7). One possible explanation for this pattern is that ridges in this climate class, which was the only sampled climate class with average $T_{min}$ values below 0 °C (Fig. A.2), experience strong winds carrying damaging ice crystals more commonly than warmer classes, and so the uniquely difficult growing environment found on ridges is made even more difficult relative to other climate classes.

A strongly context-dependent relationship was observed between landform and mean clump size. Overall, clump sizes in valleys were not significantly different than for any other landform; however, in the warmest and driest climate classes, valleys had significantly larger clumps on average. For the Xeric Mid Montane and Xeric High Montane classes the difference was approximately a factor of 2, while the Warm Dry Low Montane class, the hottest class sampled, the difference was a factor of over 100 (Fig. 7). This pattern, along with the patterns related to ridgetops discussed above, suggests that while broad conclusions about structural variation across elevation, water balance, and topography may be helpful guideposts, the signs and magnitudes of relationships between these factors and structure are not consistent across biophysical space.

The U-shaped distribution of density and basal area with increasing elevation within the six montane classes under study (Fig. 7) runs counter to the expectation that stand density should increase approximately monotonically with elevation due to the combination of orographic precipitation and longer fire return intervals (van Wagtendonk et al., 2018). This can be explained by considering actual evapotranspiration – a surrogate for productivity (Stephenson, 1998) – instead of precipitation. Actual evapotranspiration was negatively correlated with elevation for the montane climate classes ($r = -0.33$, Table 1), suggesting that lower densities in the mid-montane classes may be due to lower productivity coupled with similarly frequent fire compared to the low-montane classes. This effect was clearer than the effect of recent fire regimes. We were not able to find any statistical relationships between recent fire severity and climate classes, and fire regimes have not been reestablished long enough to test for effects of fire frequency.

One limitation to the model discussed in this section is that our study design did not fully address potential spatial autocorrelation of LMUs. Adjacent LMUs within the same or adjacent reference areas are more likely to have similar fire history, be structurally similar, and be in the same climate class. Although we did not sample enough sites to control for this factor, we suggest that, at least from a management perspective, LMUs can be considered independently.

### 4.4. Using reference condition data in forest management

The structural data for Sierra Nevada reference areas presented here are intended to be applied to forest restoration planning and treatments. The envelopes of forest structure indices (Fig. 6) can provide quantitative waypoints for interpreting current conditions and planning restoration treatments or comparing to post-treatment conditions for monitoring. Further research formalizing the inclusion of lidar-measured structure and spatial pattern into forest restoration planning is currently underway.

Evaluating departure from the reference conditions presented here is more straightforward if lidar data are available for the departed area under analysis. This allows for consistent data processing and direct comparisons between two TAO-based sets of metrics. However, the reference conditions we report can also be compared to ground-based measurements (i.e., tree lists) as long as the limitations of lidar measurements are accounted for. Specifically, each TAO may represent between one and several trees, and so measures of TAO density and clump sizes will be smaller than measures of tree density and clump sizes. For these measures our results can be taken as a lower range estimate. On the other hand, our results for basal area should be close to the actual values, since lidar accurately captures the larger trees that constitute most of the basal area (Lutz et al., 2012; Jeronimo et al., 2018). Similarly, since lidar is very effective at measuring canopy gaps our results for the open space index should be very similar to results from a field-measured stem map (Koukoulas and Blackburn, 2004).

Our results indicate that fire use has been an effective restoration tool where implemented, since the reference areas we identified are apparently set to continue burning at lower severity and are structurally similar to historical forest conditions that are thought to be resilient. Nevertheless, Sierra Nevada forest managers have been conservative in fire reintroduction and the rate of restoration lags behind regional targets (North et al., 2015; Stephens et al., 2016). This research provides strong support for increasing the use of restorative fire in the Sierra Nevada.

### 4.5. Limitations

An important drawback to using lidar measurements as the sole data source is that there are no composition data to go along with the structural measurements. Composition data must come from other sources such as modeling or imputation from structure, Landsat or other spectral data sources, or field surveys (Jeronimo et al., 2018). Lidar is also only able to characterize the shrub layer in general terms (Martinuzzi et al., 2009), which can be a problem since shrubs, as angiosperms, are a key element of mammal and bird diets in the Sierra Nevada (Lutz et al., 2014, 2017). However, the reference conditions we provide here are associated with species assemblages (Table 1). Since restoration treatments typically favor fire- and drought-tolerant species it should be clear which species will be expected for retention in a given climate class. Nevertheless, field visits and silvicultural knowledge will still be necessary to set realistic composition targets.

Another limitation of lidar is a difficulty differentiating live trees from dead trees. Some studies have used return intensity data to estimate dead tree parameters (e.g., Kim et al., 2009), but no method has yet been widely accepted and no study has been done at the TAO or equivalent scale. For these reasons we chose not to separate TAOs dominated by a live tree from TAOs dominated by a dead tree in our analyses. This may be consequential for some reference areas. For example, lidar data for areas within the Rim Fire were collected only 8–12 weeks after initial burning, probably before much of the mortality from that fire was actually discernible from lidar. We justify our inclusion of these data in two ways. Since we focused on areas that burned at low and moderate severities (1) we expect that much of the mortality was concentrated in smaller size classes, not in the larger trees that dominate TAOs, and (2) even when the measurements we report represent something closer to pre-fire structure than post-fire structure, that structure led to low and moderate severity burning and thus can be considered a desirable condition.

While the reference areas we present have experienced some fire reintroduction, they also previously experienced decades of fire suppression and other anthropogenic disturbances (e.g., grazing). We do not claim that these forests are fully restored nor that they are in the most resilient condition possible. Nevertheless, these areas have burned multiple times and are still forested with a degree of heterogeneity comparable to historical measurements. They are the best extant examples of Sierra Nevada mixed-conifer forests under an active fire regime.

In this study we have analyzed and presented results representing ranges of structure at scales of topographic facets with areas mostly around 2–20 ha. However, spatial heterogeneity in forest structure also occurs across broader scales: landscape conditions are a mix of a tree clump and canopy opening patch mosaic, shrubland and herbland covering dozens of hectares of potential forest sites, and some large aggregations of closed-canopy forest (Hessburg et al., 2005; Kane et al., 2014). Analyzing these reference areas in terms of landscape patches (e.g. seral stages *sensu* Gärtner et al., 2008) would be a valuable complement to the finer-scale data we have presented here.

## 5. Conclusions

Forest structure in active-fire landscapes is highly variable at multiple scales (Fry et al., 2014; Belote et al., 2015; Collins et al., 2016). Measuring reference conditions across contemporary active-fire landscapes using lidar affords some key advantages over historical reference conditions and field-based sampling. The Sierra Nevada region may be unique in having broad lidar coverage coupled with large areas of reintroduced fire. This allowed us to quantify landscape features over reference areas on the scale of hundreds to thousands of hectares that would not have been practically measurable with reconstruction techniques or using ground-based surveys. We captured the full range of structural variability present in the reference areas, including dense aggregations of hundreds of trees as well as large meandering openings snaking across dozens of hectares. While our novel techniques provided some new insights into forest structure under active fire conditions, our findings also confirmed past research indicating that frequent lower-severity fire leads to highly variable landscapes patterned after climatic and topographic gradients.

## Conflict of interest

None.

## Acknowledgements

Thanks to Brian Harvey, Monika Moskal, and Abby Swann for excellent guidance and advice in designing this study and preparing this manuscript. Thanks to Bob McGaughey for his continued development and collaboration on tools for measuring forest structure and pattern with lidar. Thanks to Jonathan Kane, Tristan O'Mara, Bryce Bartl-Geller, and Hailey Wiggins for assistance with lidar processing tasks. Thanks to Kendall Becker, Jamie Lydersen, and Brandon Collins for their insights and advice on criteria for identifying reference areas. Thanks to Derek Young for many thoughtful discussions about water balance modeling. Thanks to Scott Conway, Carlos Ramirez, and Hugh Safford for feedback on an earlier version of this work. Thanks to two anonymous reviewers for valuable comments that improved this manuscript.

This work was supported by the USDA Forest Service Pacific Southwest Research Station (Joint Venture Agreement 14-JV-11272139-014 "Using LiDAR to Guide Restoration in Sierra Nevada Forests" and Challenge Cost Share Agreement 13-CS-11052007-055

"Using Light Detection and Ranging (LiDAR) to Guide Burned Landscape Recovery and Restoration in Sierra Nevada Forests") and by the USDA Forest Service Colville National Forest (Joint Venture Agreement 13-JV-11062104-031 "Northeast Washington Vision 2020 Monitoring Plan"). Carnegie Airborne Observatory data collection and processing were funded by the David and Lucile Packard Foundation and the US National Park Service. The Carnegie Airborne Observatory has been made possible by grants and donations to G.P. Asner from the Avatar Alliance Foundation, Margaret A. Cargill Foundation, David and Lucile Packard Foundation, Gordon and Betty Moore Foundation, Grantham Foundation for the Protection of the Environment, W.M. Keck Foundation, John D. and Catherine T. MacArthur Foundation, Andrew Mellon Foundation, Mary Anne Nyburg Baker and G. Leonard Baker Jr., and William R. Hearst III.

## Appendix A:. Additional tables and figures

See Tables A1 and A2.

**Table A1**
Species codes, Latin names, and common names key for Table 1.

| Species code | Latin name | Common name |
|---|---|---|
| ABCO | *Abies concolor* | White fir |
| ABMA | *Abies magnifica* | Red fir |
| AECA | *Aesculus californica* | California buckeye |
| CADE | *Calocedrus decurrens* | Incense-cedar |
| JUCA | *Juniperus californica* | California juniper |
| JUOC | *Juniperus occidentalis* | Western juniper |
| LIDE | *Lithocarpus densiflorus* | Tanoak |
| PIAL | *Pinus ablicaulis* | Whitebark pine |
| PIBA | *Pinus baulforiana* | Foxtail pine |
| PICO | *Pinus contorta* | Lodgepole pine |
| PIJE | *Pinus jeffreyi* | Jeffrey pine |
| PILA | *Pinus lambertiana* | Sugar pine |
| PIMO | *Pinus monophylla* | Single-leaf pinyon |
| PIMO2 | *Pinus monticola* | Western white pine |
| PIPO | *Pinus ponderosa* | Ponderosa pine |
| PISA | *Pinus sabiniana* | Gray pine |
| PSME | *Pseudotsuga menziesii* | Douglas-fir |
| QUCH | *Quercus chrysolepis* | Canyon live oak |
| QUDO | *Quercus douglasii* | Blue oak |
| QUKE | *Quercus kelloggii* | Black oak |
| QUWI | *Quercus wislizeni* | Interior live oak |
| TSME | *Tsuga mertensiana* | Mountain hemlock |

**Table A2**
Model coefficients and statistics for height-diameter regressions on forest inventory and analysis plots within each climate class (total number of plots = 3217). Model form is dbh = $b_0$height$^{b_1}$, with dbh in cm and height in m.

| | | | | | Data used to build model | | | | | |
|---|---|---|---|---|---|---|---|---|---|---|
| Class | $b_0$ | $b_1$ | $r^2$ | RMSE (cm) | N plots | N trees | DBH min (cm) | DBH max (cm) | Height min (m) | Height max (m) |
| 1 | 1.53856 | 1.14648 | 0.64 | 3.99 | 216 | 3179 | 2.5 | 121.2 | 1.2 | 45.1 |
| 2 | 2.72283 | 1.02325 | 0.61 | 3.38 | 31 | 304 | 3.6 | 101.3 | 2.7 | 30.5 |
| 3 | 2.05648 | 1.15830 | 0.70 | 4.29 | 69 | 1310 | 2.5 | 115.1 | 0.9 | 34.4 |
| 4 | 1.14798 | 1.12029 | 0.86 | 5.09 | 21 | 654 | 2.5 | 149.6 | 2.7 | 64.6 |
| 5 | 1.37670 | 1.10943 | 0.79 | 4.73 | 460 | 13,524 | 2.5 | 209.0 | 1.8 | 68.9 |
| 6 | 1.19206 | 1.12831 | 0.86 | 5.06 | 88 | 3311 | 2.5 | 182.6 | 1.8 | 68.9 |
| 7 | 1.07742 | 1.16068 | 0.84 | 5.16 | 27 | 1091 | 2.5 | 161.0 | 2.1 | 60.4 |
| 8 | 3.03182 | 0.95797 | 0.64 | 5.64 | 30 | 723 | 2.5 | 158.2 | 1.5 | 46.3 |
| 9 | 1.44673 | 1.08746 | 0.86 | 4.74 | 335 | 13,501 | 2.5 | 203.2 | 0.9 | 70.1 |
| 10 | 1.69328 | 1.05785 | 0.86 | 5.10 | 224 | 8712 | 2.5 | 245.6 | 1.5 | 75.6 |
| 11 | 2.31671 | 1.00310 | 0.81 | 5.60 | 113 | 2251 | 2.5 | 157.5 | 1.2 | 51.8 |
| 12 | 1.40413 | 1.10804 | 0.86 | 4.78 | 62 | 2414 | 2.5 | 177.8 | 1.8 | 60.7 |
| 13 | 1.78311 | 1.04917 | 0.85 | 5.32 | 356 | 13,568 | 2.5 | 216.7 | 0.6 | 80.5 |
| 14 | 2.82546 | 0.92227 | 0.75 | 5.58 | 312 | 8589 | 2.5 | 164.6 | 0.3 | 59.4 |
| 15 | 1.93072 | 1.04232 | 0.84 | 5.77 | 127 | 4231 | 2.5 | 201.4 | 0.9 | 59.4 |
| 16 | 1.91499 | 1.06052 | 0.83 | 6.33 | 328 | 10,398 | 2.5 | 261.9 | 0.6 | 59.4 |
| 17 | 2.05270 | 1.06432 | 0.79 | 6.15 | 233 | 6498 | 2.5 | 176.8 | 0.9 | 67.1 |
| 18 | 2.58053 | 1.00908 | 0.74 | 7.68 | 164 | 5082 | 2.5 | 196.3 | 1.2 | 57.9 |
| 19 | 15.64717 | 0.67221 | 0.44 | 5.68 | 1 | 34 | 56.4 | 127.3 | 8.2 | 17.4 |
| 20 | 2.96029 | 1.02971 | 0.72 | 8.15 | 44 | 990 | 2.5 | 154.2 | 1.5 | 33.2 |

See Figs. A1 and A2.

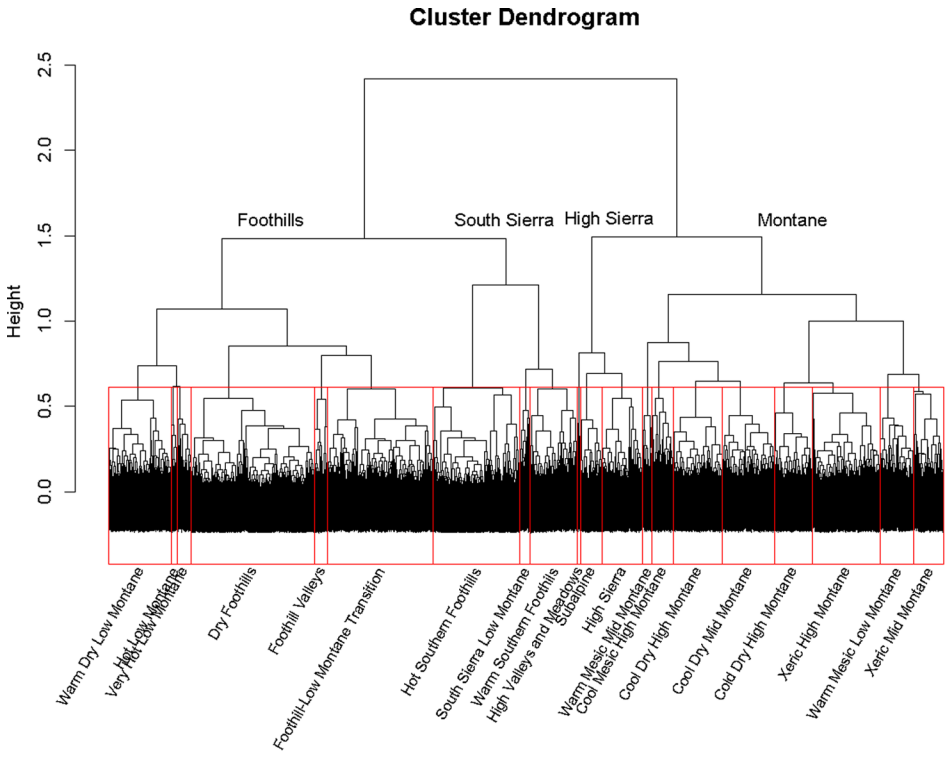


**Fig. A1.** Cluster dendrogram for climate classes. The labels at the second split indicate broad climate zones. Labels along the bottom are names of the 20 final climate classes (red boxes), interpreted by inspecting this graphic as well as Fig. A.2. (For interpretation of the references to colour in this figure legend, the reader is referred to the web version of this article.)

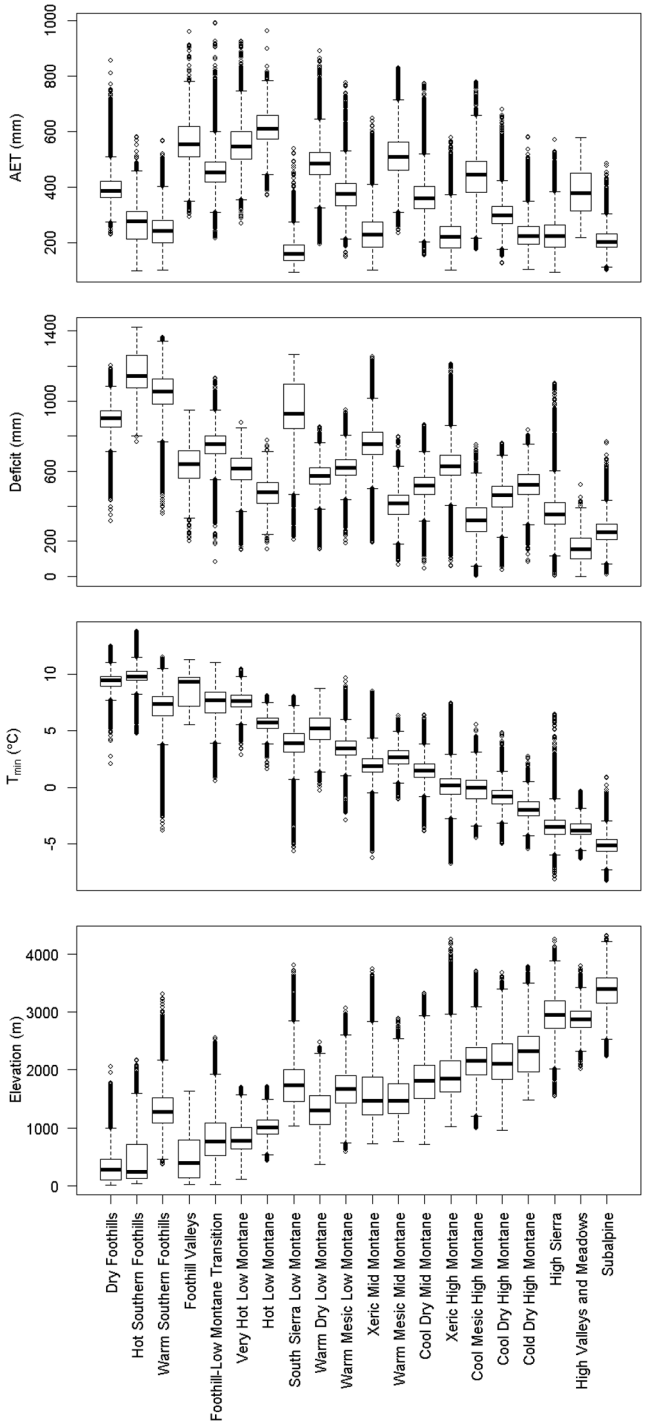


**Fig. A2.** Characteristics of the 20 climate classes in terms of actual evapotranspiration (AET), climatic water deficit (Deficit) and January minimum temperature ($T_{min}$), which were the input variables for the classification, as well as elevation, for reference. See Table 1 for class descriptions.

## Appendix B. Supplementary material

Supplementary data to this article can be found online at https://doi.org/10.1016/j.foreco.2019.01.033.

## References

Abella, S.R., Chiquoine, L.P., Sinanian, P.A., 2015. Forest change over 155 years along biophysical gradients of forest composition, environment, and anthropogenic disturbance. For. Ecol. Manage. 348, 196–207.

Asner, G.P., Knapp, D.E., Kennedy-Bowdoin, T., Jones, M.O., Martin, R.E., Boardman, J.W., Field, C.B., 2007. Carnegie airborne observatory: in-flight fusion of hyperspectral imaging and waveform light detection and ranging for three-dimensional studies of ecosystems. J. Appl. Remote Sens. 1, 013536.

Barth, M.A., Larson, A.J., Lutz, J.A., 2015. A forest reconstruction model to assess changes to Sierra Nevada mixed-conifer forest during the fire suppression era. For. Ecol. Manage. 354, 104–118.

Bechtold, W.A., Patterson, P.L., 2005. The enhanced forest inventory and analysis program: national sampling design and estimation procedures. US Department of Agriculture Forest Service, Southern Research Station Asheville, North Carolina.

Becker, K.M., Lutz, J.A., 2016. Can low-severity fire reverse compositional change in montane forests of the Sierra Nevada, California, USA? Ecosphere 7.
Belote, R.T., Larson, A.J., Dietz, M.S., 2015. Tree survival scales to community-level effects following mixed-severity fire in a mixed-conifer forest. For. Ecol. Manage. 353, 221–231.
Boynton, R., Shipley, K., Roth, N., Underwood, E., 2015. The Landscape Management Unit (LMU) Tool. URL: < http://ice.ucdavis.edu/project/landscape_management_unit_lmu_tool > (Accessed 12/1/2017).
Bray, J.R., Curtis, J.T., 1957. An ordination of the upland forest communities of Southern Wisconsin. Ecol. Monogr. 27, 325–349.
Brown, J.H., Gillooly, J.F., Allen, A.P., Savage, V.M., West, G.B., 2004. Toward a metabolic theory of ecology. Ecology 85, 1771–1789.
Cal Fire, 2018. FRAP - Data Fire Perimeters. < http://frap.fire.ca.gov/data/frapgisdata-sw-fireperimeters_download > (Accessed 12/1/2017).
Christensen, N.L., Bartuska, A.M., Brown, J.H., Carpenter, S., D'Antonio, C., Francis, R., Franklin, J.F., MacMahon, J.A., Noss, R.F., Parsons, D.J., 1996. The report of the Ecological Society of America committee on the scientific basis for ecosystem management. Ecol. Appl. 6, 665–691.
Churchill, D.J., Carnwath, G.C., Larson, A.J., Jeronimo, S.M.A., 2017. Historical forest structure, composition, and spatial pattern in dry conifer forests of the western Blue Mountains, Oregon. General Technical Report PNW-GTR-956. USDA Forest Service Pacific Northwest Research Station, Portland, OR.
Churchill, D.J., Larson, A.J., Dahlgreen, M.C., Franklin, J.F., Hessburg, P.F., Lutz, J.A., 2013. Restoring forest resilience: from reference spatial patterns to silvicultural prescriptions and monitoring. For. Ecol. Manage. 291, 442–457.
Clyatt, K.A., Crotteau, J.S., Schaedel, M.S., Wiggins, H.L., Kelley, H., Churchill, D.J., Larson, A.J., 2016. Historical spatial patterns and contemporary tree mortality in dry mixed-conifer forests. For. Ecol. Manage. 361, 23–37.
Collins, B.M., Everett, R.G., Stephens, S.L., 2011. Impacts of fire exclusion and recent managed fire on forest structure in old growth Sierra Nevada mixed-conifer forests. Ecosphere 2, 1–14.
Collins, B.M., Lydersen, J.M., Everett, R.G., Fry, D.L., Stephens, S.L., 2015. Novel characterization of landscape-level variability in historical vegetation structure. Ecol. Appl. 25, 1167–1174.
Collins, B.M., Lydersen, J.M., Fry, D.L., Wilkin, K., Moody, T., Stephens, S.L., 2016. Variability in vegetation and surface fuels across mixed-conifer-dominated landscapes with over 40 years of natural fire. For. Ecol. Manage. 381, 74–83.
Collins, B.M., Stephens, S.L., 2010. Stand-replacing patches within a 'mixed severity' fire regime: quantitative characterization using recent fires in a long-established natural fire area. Landscape Ecol. 25, 927–939.
DeRose, R.J., Long, J.N., 2014. Resistance and resilience: a conceptual framework for silviculture. For. Sci. 60, 1205–1212.
Dickinson, Y., 2014. Landscape restoration of a forest with a historically mixed-severity fire regime: What was the historical landscape pattern of forest and openings? For. Ecol. Manage. 331, 264–271.
Dobrowski, S.Z., Abatzoglou, J., Swanson, A.K., Greenberg, J.A., Mynsberge, A.R., Holden, Z.A., Schwartz, M.K., 2013. The climate velocity of the contiguous United States during the 20th century. Glob. Change Biol. 19, 241–251.
Eidenshink, J., Schwind, B., Brewer, K., Zhu, Z., Quayle, B., Howard, S., 2007. A project for monitoring trends in burn severity. Fire Ecol, vol. 3, 1, pp. 3–21. Fire Ecology Special Issue Vol 3, 4.
EPA, USGS, 2018. National Hydrography Dataset Plus Version 2. URL: < https://www.epa.gov/waterdata/nhdplus-national-hydrography-dataset-plus > (Accessed 12/1/2017).
Flint, L.E., Flint, A.L., Thorne, J.H., Boynton, R., 2013. Fine-scale hydrologic modeling for regional landscape applications: the California Basin Characterization Model development and performance. Ecol. Process. 2, 25.
Flint, L.E., Flint, A.L., Thorne, J.H., Boynton, R., 2014. 2014 California BCM (Basin Characterization Model) Downscaled Climate and Hydrology - 30-year Summaries. California Climate Commons.
Fry, D.L., Stephens, S.L., Collins, B.M., North, M.P., Franco-Vizcaíno, E., Gill, S.J., 2014. Contrasting spatial patterns in active-fire and fire-suppressed Mediterranean climate old-growth mixed conifer forests. PLoS ONE 9, e88985.
Fulé, P.Z., Covington, W.W., Moore, M.M., 1997. Determining reference conditions for ecosystem management of southwestern ponderosa pine forests. Ecol. Appl. 7, 895–908.
Gärtner, S., Reynolds, K., Hessburg, P., Hummel, S., Twery, M., 2008. Decision support for evaluating landscape departure and prioritizing forest management activities in a changing environment. For. Ecol. Manage. 256, 1666–1676.
Hagmann, R.K., Franklin, J.F., Johnson, K.N., 2013. Historical structure and composition of ponderosa pine and mixed-conifer forests in south-central Oregon. For. Ecol. Manage. 304, 492–504.
Hagmann, R.K., Franklin, J.F., Johnson, K.N., 2014. Historical conditions in mixed-conifer forests on the eastern slopes of the northern Oregon Cascade Range, USA. For. Ecol. Manage. 330, 158–170.
Hanberry, B.B., Noss, R.F., Safford, H.D., Allison, S.K., Dey, D.C., Hart, J.L., Buchanan, M.L., Cox, L.E., Dumroese, R.K., Palik, B.J., 2015. Restoration is preparation for the future. J. Forest. 113, 425–429.
Hart, J.L., Buchanan, M.L., Cox, L.E., 2015. Has forest restoration been freed from the bonds of history? J. Forest. 113, 429–430.
Hessburg, P., Reynolds, K., Salter, R., Dickinson, J., Gaines, W., Harrod, R., 2013. Landscape evaluation for restoration planning on the Okanogan-Wenatchee National Forest, USA. Sustainability 5, 805.
Hessburg, P.F., Agee, J.K., Franklin, J.F., 2005. Dry forests and wildland fires of the inland Northwest USA: contrasting the landscape ecology of the pre-settlement and modern eras. For. Ecol. Manage. 211, 117–139.
Hessburg, P.F., Churchill, D.J., Larson, A.J., Haugo, R.D., Miller, C., Spies, T.A., North, M.P., Povak, N.A., Belote, R.T., Singleton, P.H., Gaines, W.L., Keane, R.E., Aplet, G.H., Stephens, S.L., Morgan, P., Bisson, P.A., Rieman, B.E., Salter, R.B., Reeves, G.H., 2015. Restoring fire-prone Inland Pacific landscapes: seven core principles. Landscape Ecol. 30, 1805–1835.
Hessburg, P.F., Smith, B.G., Salter, R.B., 1999. Using Estimates of Natural Variation to Detect Ecologically Important Change in Forest Spatial Patterns: A Case Study, Cascade Range, Eastern Washington. Research Paper PNW-RP-514. USDA Forest Service Pacific Northwest Research Station, Portland, OR.
Heyerdahl, E.K., Loehman, R.A., Falk, D.A., 2014. Mixed-severity fire in lodgepole pine dominated forests: are historical regimes sustainable on Oregon's Pumice Plateau, USA? Can. J. For. Res. 44, 593–603.
Jeronimo, S.M.A., Kane, V.R., Churchill, D.J., McGaughey, R.J., Franklin, J.F., 2018. Applying lidar individual tree detection to management of structurally diverse forest landscapes. J. Forest. 116, 336–346.
Johnstone, J.F., Allen, C.D., Franklin, J.F., Frelich, L.E., Harvey, B.J., Higuera, P.E., Mack, M.C., Meentemeyer, R.K., Metz, M.R., Perry, G.L., 2016. Changing disturbance regimes, ecological memory, and forest resilience. Front. Ecol. Environ. 14, 369–378.
Kane, V.R., Cansler, C.A., Povak, N.A., Kane, J.T., McGaughey, R.J., Lutz, J.A., Churchill, D.J., North, M.P., 2015a. Mixed severity fire effects within the Rim fire: relative importance of local climate, fire weather, topography, and forest structure. For. Ecol. Manage. 358, 62–79.
Kane, V.R., Lutz, J.A., Cansler, C.A., Povak, N.A., Churchill, D.J., Smith, D.F., Kane, J.T., North, M.P., 2015b. Water balance and topography predict fire and forest structure patterns. For. Ecol. Manage. 338, 1–13.
Kane, V.R., Lutz, J.A., Roberts, S.L., Smith, D.F., McGaughey, R.J., Povak, N.A., Brooks, M.L., 2013. Landscape-scale effects of fire severity on mixed-conifer and red fir forest structure in Yosemite National Park. For. Ecol. Manage. 287, 17–31.
Kane, V.R., North, M.P., Lutz, J.A., Churchill, D.J., Roberts, S.L., Smith, D.F., McGaughey, R.J., Kane, J.T., Brooks, M.L., 2014. Assessing fire effects on forest spatial structure using a fusion of Landsat and airborne LiDAR data in Yosemite National Park. Remote Sens. Environ. 151, 89–101.
Kaufmann, M.R., Huckaby, L.S., Regan, C.M., Popp, J., 1998. Forest reference conditions for ecosystem management in the Sacramento Mountains, New Mexico. General Technical Report RMRS-GTR-19. USDA Forest Service, Rocky Mountain Research Station, Fort Collins, CO.
Keeley, J.E., Stephenson, N.L., 2000. Restoring natural fire regimes to the Sierra Nevada in an era of global change. In: Cole, D.N., McCool, S.F., Borrie, W.T., O'Loughlin, J. (Eds.), Wilderness science in a time of change conference Volume 5: Wilderness ecosystems, threats, and management. Proceedings. RMRS-P-15-VOL5. USDA Forest Service Rocky Mountain Research Station, Missoula, MT.
Kilgore, B.M., 1973. The ecological role of fire in Sierran conifer forests: its application to national park management. Quat. Res. 3, 496–513.
Kim, Y., Yang, Z., Cohen, W.B., Pflugmacher, D., Lauver, C.L., Vankat, J.L., 2009. Distinguishing between live and dead standing tree biomass on the North Rim of Grand Canyon National Park, USA using small-footprint lidar data. Remote Sens. Environ. 113, 2499–2510.
Knapp, E.E., Skinner, C.N., North, M.P., Estes, B.L., 2013. Long-term overstory and understory change following logging and fire exclusion in a Sierra Nevada mixed-conifer forest. For. Ecol. Manage. 310, 903–914.
Kolden, C.A., Abatzoglou, J.T., Lutz, J.A., Cansler, C.A., Kane, J.T., Van Wagtendonk, J.W., Key, C.H., 2015. Climate contributors to forest mosaics: ecological persistence following wildfire. Northwest Sci. 89, 219–238.
Koukoulas, S., Blackburn, G.A., 2004. Quantifying the spatial properties of forest canopy gaps using LiDAR imagery and GIS. Int. J. Remote Sens. 25, 3049–3072.
Langille, H.D., 1903. Forest conditions in the Cascade Range forest reserve, Oregon. United States Geological Survey, Government Printing Office, Washington, DC.
Larson, A.J., Churchill, D.J., 2012. Tree spatial patterns in fire-frequent forests of western North America, including mechanisms of pattern formation and implications for designing fuel reduction and restoration treatments. For. Ecol. Manage. 267, 74–92.
Laudenslayer, W.F., Darr, H.H., 1990. Historical effects of logging on forests of the Cascade and Sierra Nevada Ranges of California.
Leiburg, J., 1900. Cascade Range and Ashland forest reserves and adjacent regions. In: Twenty-first annual report of the United States Geological Survey to the Secretary of the United States. Government Printing Office, Washington, DC, pp. 1899–1900.
Lutz, J.A., Furniss, T.J., Germain, S.J., Becker, K.M., Blomdahl, E.M., Jeronimo, S., Cansler, C.A., Freund, J.A., Swanson, M.E., Larson, A.J., 2017. Shrub communities, spa-tial patterns, and shrub-mediated tree mortality following reintroduced fire in Yosemite National Park, California, USA. Fire Ecol. 13, 104–126.
Lutz, J.A., Furniss, T.J., Johnson, D.J., Davies, S.J., Allen, D., Alonso, A., Anderson-Teixeira, K.J., Andrade, A., Baltzer, J., Becker, K.M.L., Blomdahl, E.M., Bourg, N.A., Bunyavejchewin, S., Burslem, D.F.R.P., Cansler, C.A., Cao, K., Cao, M., Cárdenas, D., Chang, L.W., Chao, K.J., Chao, W.C., Chiang, J.M., Chu, C., Chuyong, G.B., Clay, K., Condit, R., Cordell, S., Dattaraja, H.S., Duque, A., Ewango, C.E.N., Fischer, G.A., Fletcher, C., Freund, J.A., Giardina, C., Germain, S.J., Gilbert, G.S., Hao, Z., Hart, T., Hau, B.C.H., He, F., Hector, A., Howe, R.W., Hsieh, C.F., Hu, Y.H., Hubbell, S.P., Inman-Narahari, F.M., Itoh, A., Janík, D., Kassim, A.R., Kenfack, D., Korte, L., Král, K., Larson, A.J., Li, Y., Lin, Y., Liu, S., Lum, S., Ma, K., Makana, J.R., Malhi, Y., McMahon, S.M., McShea, W.J., Memiaghe, H.R., Mi, X., Morecroft, M., Musili, P.M., Myers, J.A., Novotny, V., de Oliveira, A., Ong, P., Orwig, D.A., Ostertag, R., Parker, G.G., Patankar, R., Phillips, R.P., Reynolds, G., Sack, L., Song, G.Z.M., Su, S.H., Sukumar, R., Sun, I.F., Suresh, H.S., Swanson, M.E., Tan, S., Thomas, D.W., Thompson, J., Uriarte, M., Valencia, R., Vicentini, A., Vrška, T., Wang, X., Weiblen, G.D., Wolf, A., Wu, S.H., Xu, H., Yamakura, T., Yap, S., Zimmerman, J.K., 2018. Global importance of large-diameter trees. Glob. Ecol. Biogeogr. 27, 849–864.
Lutz, J.A., Larson, A.J., Freund, J.A., Swanson, M.E., Bible, K.J., 2013. The importance of

large-diameter trees to forest structural heterogeneity. PLoS ONE 8, e82784.
Lutz, J.A., Larson, A.J., Swanson, M.E., Freund, J.A., 2012. Ecological importance of large-diameter trees in a temperate mixed-conifer forest. PLoS ONE 7, e36131.
Lutz, J.A., Schwindt, K.A., Furniss, T.J., Freund, J.A., Swanson, M.E., Hogan, K.I., Kenagy, G.E., Larson, A.J., 2014. Community composition and allometry of Leucothoe davisiae, Cornus sericea, and Chrysolepis sempervirens. Can. J. For. Res. 44, 677–683.
Lutz, J.A., van Wagtendonk, J.W., Franklin, J.F., 2010. Climatic water deficit, tree species ranges, and climate change in Yosemite National Park. J. Biogeogr. 37, 936–950.
Lutz, J.A., Van Wagtendonk, J.W., Thode, A.E., Miller, J.D., Franklin, J.F., 2009. Climate, lightning ignitions, and fire severity in Yosemite National Park, California, USA. Int. J. Wildland Fire 18, 765–774.
Lydersen, J., North, M., 2012. Topographic variation in structure of mixed-conifer forests under an active-fire regime. Ecosystems 15, 1134–1146.
Lydersen, J.M., Collins, B.M., Brooks, M.L., Matchett, J.R., Shive, K.L., Povak, N.A., Kane, V.R., Smith, D.F., 2017. Evidence of fuels management and fire weather influencing fire severity in an extreme fire event. Ecol. Appl. 27, 2013–2030.
Lydersen, J.M., North, M.P., Collins, B.M., 2014. Severity of an uncharacteristically large wildfire, the Rim Fire, in forests with relatively restored frequent fire regimes. For. Ecol. Manage. 328, 326–334.
Lydersen, J.M., North, M.P., Knapp, E.E., Collins, B.M., 2013. Quantifying spatial patterns of tree groups and gaps in mixed-conifer forests: reference conditions and long-term changes following fire suppression and logging. For. Ecol. Manage. 304, 370–382.
Mallek, C., Safford, H., Viers, J., Miller, J., 2013. Modern departures in fire severity and area vary by forest type, Sierra Nevada and southern Cascades, California, USA. Ecosphere 4, 1–28.
Martinuzzi, S., Vierling, L.A., Gould, W.A., Falkowski, M.J., Evans, J.S., Hudak, A.T., Vierling, K.T., 2009. Mapping snags and understory shrubs for a LiDAR-based assessment of wildlife habitat suitability. Remote Sens. Environ. 113, 2533–2546.
McCune, B., Grace, J.B., Urban, D.L., 2002. Analysis of ecological communities. MjM software design Gleneden Beach, OR.
McGaughey, R.J., 2018. FUSION/LDV: Software for LIDAR Data Analysis and Visualization: Version 3.70. USDA Forest Service Pacific Northwest Research Station, Seattle, WA.
Meddens, A.J., Kolden, C.A., Lutz, J.A., Smith, A., Cansler, C.A., Abatzoglou, J.T., Meigs, G.W., Downing, W.M., Krawchuk, M.A., 2018. Fire Refugia: what are they, and why do they matter for global change? Bioscience.
Meigs, G.W., Krawchuk, M.A., 2018. Composition and Structure of Forest Fire Refugia: what are the ecosystem legacies across burned landscapes? Forests 9, 243.
Millar, C.I., Woolfenden, W.B., 1999. The role of climate change in interpreting historical variability. Ecol. Appl. 9, 1207–1216.
Moore, M.M., Wallace Covington, W., Fule, P.Z., 1999. Reference conditions and ecological restoration: a southwestern ponderosa pine perspective. Ecol. Appl. 9, 1266–1277.
Munger, T.T., 1912. The future yield of yellow pine stands in Oregon. Unpublished report. Transcript of archived original available from fs.usda.gov/detail/umatilla/learning/history-culture. In. Government Printing Office, Washington, DC.
North, M., Collins, B.M., Stephens, S., 2012. Using fire to increase the scale, benefits, and future maintenance of fuels treatments. J. Forest. 110, 392–401.
North, M., Innes, J., Zald, H., 2007. Comparison of thinning and prescribed fire restoration treatments to Sierran mixed-conifer historic conditions. Can. J. For. Res. 37, 331–342.
North, M., Stine, P., O'Hara, K., Zielinski, W., Stephens, S., 2009. An ecosystem management strategy for Sierran mixed-conifer forests, General Technical Report PSW-GTR-220. USDA Forest Service Pacific Southwest Research Station, Albany, CA.
North, M.P., Kane, J.T., Kane, V.R., Asner, G.P., Berigan, W., Churchill, D.J., Conway, S., Gutiérrez, R.J., Jeronimo, S., Keane, J., Koltunov, A., Mark, T., Moskal, M., Munton, T., Peery, Z., Ramirez, C., Sollmann, R., White, A., Whitmore, S., 2017. Cover of tall trees best predicts California spotted owl habitat. For. Ecol. Manage. 405, 166–178.
North, M.P., Stephens, S.L., Collins, B.M., Agee, J.K., Aplet, G., Franklin, J.F., Fulé, P.Z., 2015. Reform forest fire management. Science 349, 1280–1281.
Oksanen, J., Blanchet, F.G., Kindt, R., Legendre, P., Minchin, P.R., O'Hara, R.B., Simpson, G.L., Solymos, P., Stevens, M.H.H., Wagner, H., 2016. vegan: Community Ecology Package.
Parsons, D.J., Botti, S.J., 1996. Restoration of Fire in National Parks. In: Hardy, C.C., Arno, S.F. (Eds.), The use of fire in forest restoration. General Technical Report INT-GTR-341. USDA Forest Service Intermountain Research Station, Ogden, UT.
Parsons, D.J., van Wagtendonk, J.W., 1996. Fire research and management in the Sierra Nevada National Parks. Science and ecosystem management in the national parks. University of Arizona Press, Tucson, Arizona, USA, 25-48.
Core Team, R., 2016. R: A language and environment for statistical computing. R Foundation for Statistical Computing, Vienna, Austria.
Safford, H.D., Stevens, J.T., 2017. Natural range of variation for yellow pine and mixed-conifer forests in the Sierra Nevada, southern Cascades, and Modoc and Inyo National Forests, California, USA. Gen. Tech. Rep. PSW-GTR-256. Albany, CA: US Department of Agriculture, Forest Service, Pacific Southwest Research Station. 229 p. 256.
Safford, H.D., Van de Water, K.M., 2014. Using fire return interval departure (FRID) analysis to map spatial and temporal changes in fire frequency on national forest lands in California. Res. Pap. PSW-RP-266. Albany, CA: US Department of Agriculture, Forest Service, Pacific Southwest Research Station. 59 p 266.
Schneider, E.E., Sánchez Meador, A.J., Covington, W.W., 2015. Reference conditions and historical changes in an unharvested ponderosa pine stand on sedimentary soil. Reestor. Ecol. 24, 212–221.
Scholl, A.E., Taylor, A.H., 2010. Fire regimes, forest change, and self-organization in an old-growth mixed-conifer forest, Yosemite National Park, USA. Ecol. Appl. 20, 362–380.
Seidl, R., Spies, T.A., Peterson, D.L., Stephens, S.L., Hicke, J.A., 2015. Searching for resilience: addressing the impacts of changing disturbance regimes on forest ecosystem services. J. Appl. Ecol. 53, 120–129.
Skinner, C.N., Chang, C., 1996. Fire regimes, past and present. In, Sierra Nevada Ecosystem Project: Final report to Congress, vol II. Assessments and scientific basis for management options. University of California Center for Water and Wildland Resources, Davis, California.
Stephens, S.L., Agee, J.K., Fulé, P., North, M., Romme, W., Swetnam, T., Turner, M.G., 2013. Managing forests and fire in changing climates. Science 342, 41–42.
Stephens, S.L., Collins, B.M., Biber, E., Fulé, P.Z., 2016. US federal fire and forest policy: emphasizing resilience in dry forests. Ecosphere 7, e01584.
Stephens, S.L., Lydersen, J.M., Collins, B.M., Fry, D.L., Meyer, M.D., 2015. Historical and current landscape-scale ponderosa pine and mixed conifer forest structure in the Southern Sierra Nevada. Ecosphere 6, 1–63.
Stephens, S.L., Millar, C.I., Collins, B.M., 2010. Operational approaches to managing forests of the future in Mediterranean regions within acontext of changing climates. Environ. Res. Lett. 5, 024003.
Stephens, S.L., Ruth, L.W., 2005. Federal forest-fire policy in the United States. Ecol. Appl. 15, 532–542.
Stephenson, N., 1998. Actual evapotranspiration and deficit: biologically meaningful correlates of vegetation distribution across spatial scales. J. Biogeogr. 25, 855–870.
Taylor, A.H., 2010. Fire disturbance and forest structure in an old-growth Pinus ponderosa forest, southern Cascades, USA. J. Veg. Sci. 21, 561–572.
Underwood, E.C., Viers, J.H., Quinn, J.F., North, M., 2010. Using topography to meet wildlife and fuels treatment objectives in fire-suppressed landscapes. Environ. Manage. 46, 809–819.
USDA Forest Service, 2018. FSGeodata Clearinghouse. URL: < https://data.fs.usda.gov/geodata/edw/datasets.php > (Accessed 2/20/2018).
Vale, T., 2013. Fire, Native Peoples, and the Natural Landscape. Island Press.
Van de Water, K., North, M., 2011. Stand structure, fuel loads, and fire behavior in riparian and upland forests, Sierra Nevada Mountains, USA; a comparison of current and reconstructed conditions. For. Ecol. Manage. 262, 215–228.
van Wagtendonk, J.W., 1994. Spatial patterns of lightning strikes and fires in Yosemite National Park. In: Proceedings of the 12th Conference on Fire and Forest Meteorology, pp. 223–231.
van Wagtendonk, J.W., 2007. The history and evolution of wildland fire use. Fire Ecol. 3, 3–17.
van Wagtendonk, J.W., Cayan, D.R., 2008. Temporal and spatial distribution of lightning strikes in California in relation to large-scale weather patterns. Fire Ecol. 4, 34–56.
van Wagtendonk, J.W., Fites-Kaufman, J.A., Safford, H.D., North, M.P., Collins, B.M., 2018. Sierra Nevada bioregion. In: van Wagtendonk, J.W., Sugihara, N.G., Stephens, S.L., Thode, A.D., Shaffer, K.E., Fites-Kaufman, J.A. (Eds.), Fire in California's Ecosystems. University of California Press, Oakland, CA, pp. 249–278.
van Wagtendonk, J.W., Lutz, J.A., 2007. Fire regime attributes of wildland fires in Yosemite National Park, USA. Fire Ecology 3, 34–52.
van Wagtendonk, J.W., van Wagtendonk, K.A., Thode, A.E., 2012. Factors associated with the severity of intersecting fires in Yosemite National Park, California, USA. Fire Ecol. 8, 11–31.
Wiggins, H.L., 2017. The influence of tree height on lidar's ability to accurately characterize forest structure and spatial pattern across reference landscapes. Master of Science Thesis. University of Montana, Missoula, MT.